

Electronic structure calculations for solids with application to NMR spectroscopy

Gilles de Wijs

Theoretical Chemistry, Institute for Molecules and Materials, Radboud University

December 2017

Radboud University Nijmegen



Acknowledgments VASP

VASP:

Martijn Marsman
Georg Kresse

ESM:

Filipe Vasconcelos

RUG:

Remco Havenith

Others:

T. Thonhauser
D. Ceresoli
D. Vanderbilt

Funding:

FOM
NCF



Radboud University Nijmegen



Outline

- Density functional theory in a nutshell
- DFT modelling of NMR parameters... in solids: historical overview
- Literature summary
- Plane waves & pseudopotentials
- Basics of the projector-augmented wave (PAW) method
- Calculating electric field gradients (EFGs) with PAW
- Basics of chemical shielding
- AE theory of chemical shielding
- Basic GIPAW
- A simple molecular method
- GIPAW linear response for solids
- Illustration on cubic carbon
- Converse approach to shielding (general)
- Modern theory of orbital magnetization
- Converse approach to shielding (GIPAW for crystals)
- Benchmarks, VASP & FLAPW (WIEN2k) & GIAO (Dalton)
- GIPAW 2-centre corrections.
- Doing a calculation.
- Illustrations:
 - Modelling EFGs in (disordered) $\text{Al}_x\text{Ga}_{1-x}\text{As}$ & InGaP & (maybe) MAPbI_3
 - Shieldings: exploring accuracy and chemical interactions in organic crystals, PPTA and/or Venlafaxine and/or Isocyanocarbazole and/or DL-aminoheptanoic acid

Density functional theory

Hohenberg-Kohn-Sham in a tiny nutshell

The world consists of positive nuclei, and electrons. The electronic ground state energy and density can be obtained by minimizing a functional of the density. To approximate the density functional, fictitious Kohn-Sham orbitals are introduced. This allows for a good kinetic energy. Exchange and correlation (XC) energies are parametrized from, e.g., numerical exact uniform gas data (LDA). The functional is minimized under the constraint of orthonormal orbitals. The EL equations define a new, *self-consistent*, Kohn-Sham Hamiltonian:

$$\rho(\mathbf{r}) = \sum_n^{\text{occ}} |\psi_n(\mathbf{r})|^2, \quad H|\psi_n\rangle = \left(\frac{p^2}{2m} + V_{\text{Coulomb}}^{\text{e-e}}(\rho) + V_{\text{Coulomb}}^{\text{e-nuclei}} + V_{\text{xc}} \right) |\psi_n\rangle = \epsilon_n |\psi_n\rangle$$

Many flavours of XC exist... various gradient-corrected functiontials (PW91, PBE, etc.) or hybrids mixed with HF (B3LYP, HSE, etc.).

For an introduction: R.M. Martin, Electronic Structure, Cambridge University Press (2004), ISBN 0 521 78285 6

DFT modeling of NMR parameters: overview

Incomplete history of DFT in Solid State NMR

Here “solid state” means “crystal” means “periodic lattice”

1980's: EFGs in FLAPW, Blaha, Schwarz, Herzig

1990's: shielding basics, Mauri, Louie, et al.

1999: EFGs in PAW, Petrilli, Blöchl, et al.

1999: decouple core from valence shielding, Gregor, Mauri & Car

2001: GIPAW method, Pickard & Mauri

2001: pseudopotential approach to shielding, Sebastiani & Parrinello

2005: Modern theory of orbital magnetisation, Thonhauser, Ceresoli, Vanderbilt, Resta, ...

2009: converse approach to shielding, Thonhauser, Vanderbilt, et al.

(Incomprehensive) Literature Summary I

General Solid State electronic structure

R.M. Martin, Electronic Structure, Basic Theory and Practical Methods, Cambridge University Press (2004).

E. Kakiras, Atomic and Electronic Structure of Solids, Cambridge University Press (2003).

VASP

http://cms.mpi.univie.ac.at/vasp-workshop/slides/*.pdf

Chemical Shielding

Quantum-chemistry methods

T. Helgaker, M. Jaszunski, and K. Ruud, Chem. Rev. **99**, 293 (1999)

Solids - Basic theory

F. Mauri, B.G. Pfrommer, and S.G. Louie, Phys. Rev. Lett. **77**, 5300 (1996)

F. Mauri, and S.G. Louie, Phys. Rev. Lett. **76**, 4246 (1996)

T. Gregor, F. Mauri, and R. Car, J. Chem. Phys. **111** 1815 (1999)

GIPAW linear response

G.J. Pickard, and F. Mauri, Phys. Rev. B **63**, 245101 (2001)

J.R. Yates, G.J. Pickard, and F. Mauri, Phys. Rev. B **76**, 024401 (2007)

GIPAW heavy nuclei (ZORA):

J.R. Yates, C.J. Pickard, M.C. Payne, and F. Mauri, J. Chem. Phys. **118**, 5746 (2003)

GIPAW & converse

T. Thonhauser, D. Ceresoli, A.A. Mostofi, N. Marzari, R. Resta, and D. Vanderbilt, J. Chem. Phys. **131**, 101101 (2009)

D. Ceresoli, N. Marzari, M.G. Lopez, and T. Thonhauser, Phys. Rev. B **81**, 184424 (2010)

(Incomprehensive) Literature Summary II

D. Ceresoli, T. Thonhauser, D. Vanderbilt, and R. Resta, Phys. Rev. B **74**, 024408 (2006)

FLAPW

R. Laskowski, and P. Blaha, Phys. Rev. B **85** 035132 (2012)

R. Laskowski, and P. Blaha, Phys. Rev. B **89** 014402 (2014)

Wannier & pseudopotentials

D. Sebastiani, and M. Parrinello, J. Phys. Chem. A **105**, 1951 (2001)

ADF

D. Skachkov, M. Krykunov, E. Kadantsev, and T. Ziegler,

J. Chem. Theory Comput. **6**, 1650 (2010)

D. Skachkov, M. Krykunov, and T. Ziegler, Can. J. Chem. **89**, 1150 (2011)

VASP

F. Vasconcelos, G.A. de Wijs, R.W.A. Havenith, M. Marsman, G. Kresse,

J. Chem. Phys. **139**, 014109 (2013)

G.A. de Wijs, R. Laskowski, P. Blaha, R.A.W. Havenith, G. Kresse, M. Marsman,

J. Chem. Phys. **146**, 064115 (2017)

Vibrational effects

S. Rossano, F. Mauri, C.J. Pickard, and I. Farnan, J. Phys. Chem. B **109**, 7245 (2005)

B. Monserrat, R.J. Needs, C.J. Pickard, J. Chem. Phys. **141**, 134113 (2014)

Other NMR properties, background reading

Metals, Knight shift

M. d'Avezac, N. Marzari, and F. Mauri, Phys. Rev. B **76**, 165122 (2007)

(Incomprehensive) Literature Summary III

J-coupling

S.A. Joyce, J.R. Yates, C.J. Pickard and F. Mauri, *J. Chem. Phys.* **127**, 204107 (2007)

EFG-PAW

H.M. Petrilli, P.E. Blöchl, P. Blaha, and K. Schwarz, *Phys. Rev. B* **57**, 14690 (1998)

EFG-FLAPW

P. Blaha, K. Schwarz, and P. Herzig, *Phys. Rev. Lett.* **54**, 1192 (1985)

P. Dufek, P. Blaha, and K. Schwarz, *Phys. Rev. Lett.* **75**, 3545 (1995)

PAW

P.E. Blöchl, *Phys. Rev. B* **50**, 17953 (1994)

G. Kresse, and D. Joubert, *Phys. Rev. B* **59**, 1758 (1999)

GIPAW NMR review

T. Charpentier, *Solid State Nucl. Magn. Reson.* **40**, 1 (2011)

S.E. Ashbrook, and D. McKay, *Chem. Commun.* **52**, 7186 (2016)

Lattice basics I

We are dealing with crystals. After each translation over a lattice vector

$$\mathbf{R} = n_1 \mathbf{a}_1 + n_2 \mathbf{a}_2 + n_3 \mathbf{a}_3$$

we see the same nuclei and electron charge density. \mathbf{a}_1 , \mathbf{a}_2 and \mathbf{a}_3 are the *primitive* lattice vectors.

We can set up a *reciprocal lattice*:

$$\mathbf{G} = m_1 \mathbf{G}_1 + m_2 \mathbf{G}_2 + m_3 \mathbf{G}_3$$

where the three basis vectors are:

$$\mathbf{G}_1 = 2\pi \frac{\mathbf{a}_2 \times \mathbf{a}_3}{\mathbf{a}_1 \cdot (\mathbf{a}_2 \times \mathbf{a}_3)} , \quad \mathbf{G}_2 = 2\pi \frac{\mathbf{a}_3 \times \mathbf{a}_1}{\mathbf{a}_1 \cdot (\mathbf{a}_2 \times \mathbf{a}_3)} , \quad \mathbf{G}_3 = 2\pi \frac{\mathbf{a}_1 \times \mathbf{a}_2}{\mathbf{a}_1 \cdot (\mathbf{a}_2 \times \mathbf{a}_3)}$$

$$\text{so that : } \mathbf{a}_i \cdot \mathbf{G}_j = 2\pi \delta_{ij} \quad (1 \leq i, j \leq 3)$$

Lattice basics II

Any cell-periodic function f can now be expanded:

$$f(\mathbf{r}) = \sum_{\mathbf{G}} c_{\mathbf{G}} e^{i\mathbf{G} \cdot \mathbf{r}}, \quad f(\mathbf{r} + \mathbf{R}) = \sum_{\mathbf{G}} c_{\mathbf{G}} e^{i\mathbf{G} \cdot \mathbf{r}} \underbrace{e^{i\mathbf{G} \cdot \mathbf{R}}}_1 = f(\mathbf{r})$$

The functions ($\Omega = |\mathbf{a}_1 \cdot (\mathbf{a}_2 \times \mathbf{a}_3)|$ is the unit cell volume)

$$\frac{1}{\sqrt{\Omega}} e^{i\mathbf{G} \cdot \mathbf{r}}$$

are orthonormal (in the unit cell). Now i and j label all reciprocal lattice vectors:

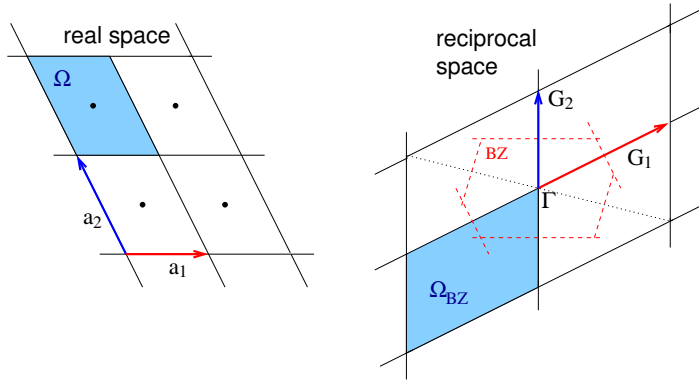
$$\int \left(\frac{1}{\sqrt{\Omega}} e^{i\mathbf{G}_i \cdot \mathbf{r}} \right)^* \frac{1}{\sqrt{\Omega}} e^{i\mathbf{G}_j \cdot \mathbf{r}} d\mathbf{r} = \frac{1}{\Omega} \int e^{i(\mathbf{G}_j - \mathbf{G}_i) \cdot \mathbf{r}} d\mathbf{r} = \begin{cases} \Omega/\Omega = 1 & \text{if } \mathbf{G}_i = \mathbf{G}_j \\ 0 & \text{if } \mathbf{G}_i - \mathbf{G}_j = \mathbf{G}_k \neq 0 \end{cases}$$

Note that:

$$c_{-\mathbf{G}} = c_{\mathbf{G}}^*$$

Lattice basics III

Let's have a little picture:



Note the Wigner Seitz construction to construct the Brillouin zone (BZ).

The reciprocal lattice of bcc (fcc) is fcc (bcc). $\Omega_{BZ} = (2\pi)^3 / \Omega$.

Bloch I

Consider all possible translations $T_{\mathbf{R}}$ that map the lattice onto itself.

$$T_{\mathbf{R}}\Phi(\mathbf{r}) = \Phi(\mathbf{r} + \mathbf{R})$$

The Kohn-Sham Hamiltonian commutes with all $T_{\mathbf{R}}$, $[H_{\text{KS}}, T_{\mathbf{R}}] = 0$. Also $[T_{\mathbf{R}}, T_{\mathbf{R}'}] = 0$. Hence the eigenstates can be chosen to diagonalize all operators. So we consider the eigenstates and eigenvalues of $T_{\mathbf{R}}$:

$$T_{\mathbf{R}}\Phi(\mathbf{r}) = c(\mathbf{R})\Phi(\mathbf{r})$$

Consider consecutive translations:

$$T_{\mathbf{R}} T_{\mathbf{R}'} = T_{\mathbf{R}+\mathbf{R}'} \Rightarrow c(\mathbf{R} + \mathbf{R}') = c(\mathbf{R})c(\mathbf{R}')$$

A breakdown in primitive translations

$$\mathbf{R} = n_1 \mathbf{a}_1 + n_2 \mathbf{a}_2 + n_3 \mathbf{a}_3$$

gives:

$$c(\mathbf{R}) = c(\mathbf{a}_1)^{n_1} c(\mathbf{a}_2)^{n_2} c(\mathbf{a}_3)^{n_3}$$

Bloch II

Now consider the Ansatz:

$$c(\mathbf{R}) = e^{i\mathbf{k}\cdot\mathbf{R}} \text{ with } \mathbf{k} = x_1 \mathbf{G}_1 + x_2 \mathbf{G}_2 + x_3 \mathbf{G}_3$$

Just complete:

$$\begin{aligned} c(\mathbf{R}) &= e^{i\mathbf{k}\cdot\mathbf{R}} = e^{i(x_1 \mathbf{G}_1 + x_2 \mathbf{G}_2 + x_3 \mathbf{G}_3) \cdot (n_1 \mathbf{a}_1 + n_2 \mathbf{a}_2 + n_3 \mathbf{a}_3)} \\ &= (e^{2\pi i x_1})^{n_1} (e^{2\pi i x_2})^{n_2} (e^{2\pi i x_3})^{n_3} = c(\mathbf{a}_1)^{n_1} c(\mathbf{a}_2)^{n_2} c(\mathbf{a}_3)^{n_3} \end{aligned}$$

So we solved for $c(\mathbf{R})$, where $c(\mathbf{a}_1)$, $c(\mathbf{a}_2)$ and $c(\mathbf{a}_3)$ are determined by the location in the BZ. So we have Bloch's theorem:

$$\Phi_{n\mathbf{k}}(\mathbf{r} + \mathbf{R}) = e^{i\mathbf{k}\cdot\mathbf{R}} \Phi_{n\mathbf{k}}(\mathbf{r})$$

For convenience we also put a band index. It can also be formulated as:

$$\Phi_{n\mathbf{k}}(\mathbf{r}) = e^{i\mathbf{k}\cdot\mathbf{r}} u_{n\mathbf{k}}(\mathbf{r})$$

where $u_{n\mathbf{k}}(\mathbf{r})$ is a periodic function on the lattice (so can be expanded on the reciprocal lattice).

Born-Von Karman boundary condition I

Impose super-periodicity on the orbitals ($1 \leq i \leq 3$):

$$\Phi(\mathbf{r} + N_i \mathbf{a}_i) = \Phi(\mathbf{r})$$

Bloch:

$$\Phi_{\mathbf{k}}(\mathbf{r} + N_i \mathbf{a}_i) = e^{i\mathbf{k} \cdot N_i \mathbf{a}_i} \Phi_{\mathbf{k}}(\mathbf{r})$$

Choose direction i :

$$N_i \mathbf{k} \cdot \mathbf{a}_i = 2\pi m \Leftarrow \mathbf{k} = \frac{m}{N_i} \mathbf{G}_i$$

We can add any linear combination of the other two reciprocal lattice vectors ... so to satisfy all three constraints:

$$\mathbf{k} = \frac{m_1}{N_1} \mathbf{G}_1 + \frac{m_2}{N_2} \mathbf{G}_2 + \frac{m_3}{N_3} \mathbf{G}_3$$

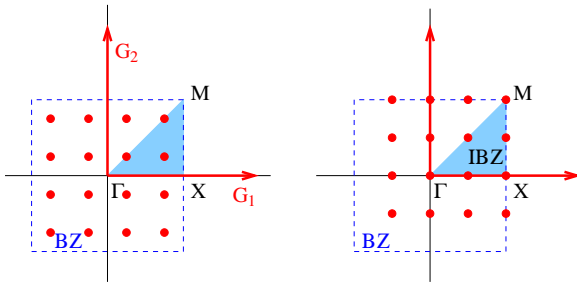
This puts a “grid” in the BZ. A \mathbf{k} -space volume $(2\pi)^3 / (\Omega N_1 N_2 N_3)$ is associated with each state. We need $N_i \rightarrow \infty$ to describe the infinite lattice.

Integrating the Brillouin Zone I

We often have to integrate over the BZ. Typically it looks like:

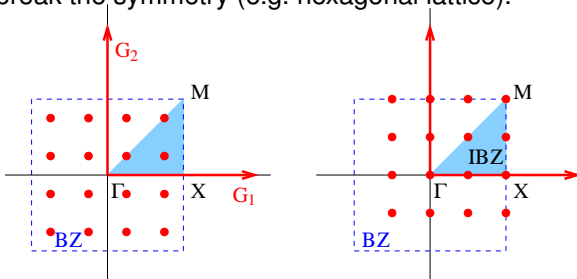
$$\sum_n \frac{\Omega}{(2\pi)^3} \int_{BZ} f_{n\mathbf{k}} d\mathbf{k}$$

One approximates with a sum over points in the BZ. In the Monkhorst & Pack method (Phys. Rev. B **13**, 5188 (1976)), one sums over a grid (cf. Born-Von Karman).



Integrating the Brillouin Zone II

The grid can be either centered on or (symmetrically) around Γ . The latter can break the symmetry (e.g. hexagonal lattice).



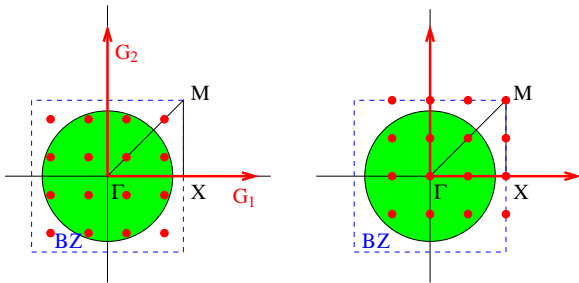
You want the mesh so fine that the integral is converged.

One typically uses symmetry to replace the sum by a weighted sum over the IBZ (irreducible BZ). In the SCF cycle one constructs the charge density as:

$$\rho(\mathbf{r}) = \sum_n \sum_{\mathbf{k} \in \text{BZ}} w_{\mathbf{k}} f_{n\mathbf{k}} \rho_{n\mathbf{k}}(\mathbf{r})$$

and then, e.g., symmetrizes $\rho(\mathbf{r})$, etc.

Integrating the Brillouin Zone III



For our systems (insulators and semi-conductors) we have a gap. For metals, bands can cross the Fermi surface: $f_{n\mathbf{k}}$ can make a very sharp drop. Hence one needs a very fine mesh. To work around this: smearing methods. These are typically geared towards fast convergence of the total energy (e.g., Methfessel-Paxton, tetrahedra with Blöchl correction), but can also be very useful to make good density of states pictures (linear tetrahedron method).

Plane waves as a basis I

We have seen that plane waves are a natural basis for cell-periodic functions, so for the cell-periodic part of the Bloch states and for the charge density:

$$u_{n\mathbf{k}}(\mathbf{r}) = \sum_{\mathbf{G}} c_{n\mathbf{k}\mathbf{G}} e^{i\mathbf{G} \cdot \mathbf{r}}, \quad \rho(\mathbf{r}) = \sum_{\mathbf{G}} c_{\mathbf{G}} e^{i\mathbf{G} \cdot \mathbf{r}}$$

These basis sets are truncated for sufficiently fast \mathbf{G} :

$$\frac{\hbar^2 |\mathbf{G} + \mathbf{k}|^2}{2m_e} < E_{\text{kin,cut}}^{(u)}, \quad \frac{\hbar^2 |\mathbf{G}|^2}{2m_e} < E_{\text{kin,cut}}^{(\rho)}$$

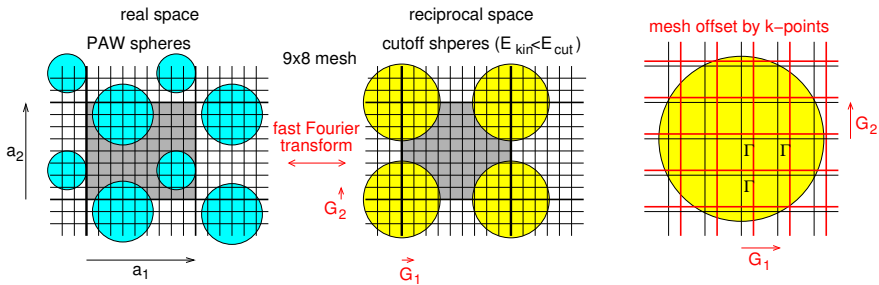
So we only consider basis functions within the *cutoff sphere*, with energies less than the *kinetic energy cutoff*.

If we introduce an artificial periodicity in reciprocal space we can use FFTs to go between real and reciprocal space meshes.

These brings huge computational benefits. E.g., the kinetic energy becomes trivial, we can remove the nasty convolution in the Hartree energy, ...

Plane waves as a basis II

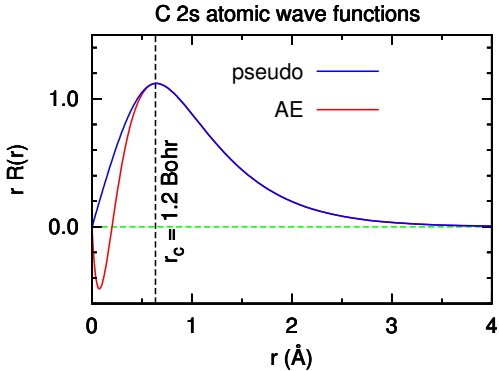
$$\Phi_{n\mathbf{k}}(\mathbf{r}) = e^{i\mathbf{k}\cdot\mathbf{r}} u_{n\mathbf{k}}(\mathbf{r}) = e^{i\mathbf{k}\cdot\mathbf{r}} \sum_{\mathbf{G}} c_{n\mathbf{k}\mathbf{G}} e^{i\mathbf{G}\cdot\mathbf{r}}, \quad \rho(\mathbf{r}) = \sum_{\mathbf{G}} c_{\mathbf{G}} e^{i\mathbf{G}\cdot\mathbf{r}}$$



Via a (fast) Fourier transform, the \mathbf{G} space expansion corresponds to the grid in real space.

Near the atomic cores (blue spheres) converging the basis is extremely cumbersome... pseudopotentials or PAW.

Plane waves & pseudopotentials I



Recipe: Take a frozen core. Remove the core electrons from the calculation. *Construct pseudo KS states that are smoothed within a radius r_c . Construct pseudopotentials that have the pseudo states as solution (“unscreening”). Use the smooth PP for your actual calculation.*

The *red part* is done on the isolated atom.

Plane waves & pseudopotentials II

Scattering approach: solutions for the interstitial region are matched via the logarithmic derivates at the radius r_c . PP approach: match the pseudo $\tilde{\phi}_I$ and real (“all-electron”) ϕ_I states via the logarithmic derivates at r_c .

$$\frac{\partial \ln \phi_I(r, \epsilon)}{\partial r} \Big|_{r=r_c} = \frac{\partial \ln \tilde{\phi}_I(r, \epsilon)}{\partial r} \Big|_{r=r_c}$$

Norm-conservation (NC):

$$\int_0^{r_c} |\phi_I(r, \epsilon)|^2 r^2 dr = \int_0^{r_c} |\tilde{\phi}_I(r, \epsilon)|^2 r^2 dr$$

NC insures scattering is correct in first order:

$$\frac{\partial}{\partial \epsilon} \frac{\partial \ln \phi_I(r, \epsilon)}{\partial r} \Big|_{r=r_c} = \frac{\partial}{\partial \epsilon} \frac{\partial \ln \tilde{\phi}_I(r, \epsilon)}{\partial r} \Big|_{r=r_c}$$

NC makes PPs “hard” (relatively high energy cutoff). It can be relieved, with ultra-soft PPs and PAW, the price is an overlap matrix S (see later...).

Plane waves & pseudopotentials III

Back to the recipe. To make a PP:

1. Do a (numerically exact) exact all-electron (AE) calculation for a reference atom (in a reference state).
2. Select pseudization energies ϵ_{nl} (n numbers the energies per angular momentum channel l).
3. Replace AE orbitals with NC pseudo orbitals (continuity of orbitals and derivatives at r_c)
4. Unscreen and obtain the PP.

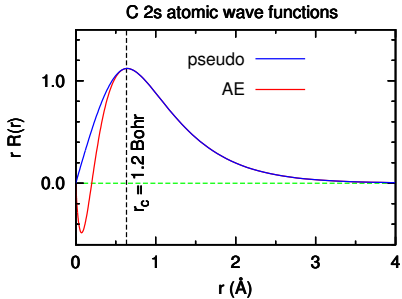
Typically the PP can be cast as:

$$V_{\text{loc}} + \sum_{ij} |\tilde{p}_i\rangle D_{ij} \langle \tilde{p}_j|$$

where $i(j)$ is a compounded index: I, m, n . The $|\tilde{p}_i\rangle$ are short range. V_{loc} has the Coulomb tail.

Don't try this at home: You'll have either ghost states or just bad scattering properties & transferability. Leave it to an expert.

Plane waves & pseudopotentials IV



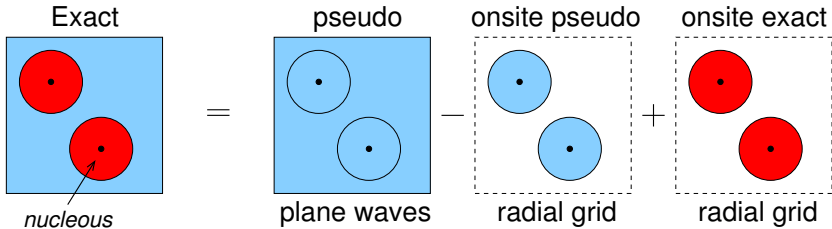
With pseudopotentials you loose information on the orbitals near the nuclei. That's fine for most properties.

For magnetic materials you need to be very careful.

For NMR-observables you can get meaningful results only in a few cases in the top part of the periodic table (very hard PP for, e.g., hydrocarbons).

Basics of the PAW method I

Projector Augmented Wave method (Blöchl 1994): An all-electron (AE) method with pseudopotential “simplicity”. It is **not a pseudopotential method**. Key approximation: **frozen core** (can be partly relaxed).



The AE states are reconstructed, replacing a pseudo by an AE partial wave: **Correct shape of KS states near nucleus**. Only *one-centre* corrections of *short range* ($r \leq r_c$).

P.E. Blöchl, Phys. Rev. B **50**, 17953 (1994).

Basics of the PAW method II

A linear transformation between pseudo and AE KS states:

$$|\Phi_a\rangle = |\tilde{\Phi}_a\rangle + \sum_{\mathbf{R}i} (|\phi_{\mathbf{R}i}\rangle - |\tilde{\phi}_{\mathbf{R}i}\rangle) \langle \tilde{p}_{\mathbf{R}i} | \tilde{\Phi}_a \rangle$$

Here $i = n, l, m$. The projector functions \tilde{p}_i and partial waves $\tilde{\phi}_i$ are “complete”:

$$\langle \tilde{p}_i | \tilde{\phi}_j \rangle = \delta_{ij}$$

The partial waves are constructed in an atomic calculation. Frozen core electrons are removed from the problem. An effective “pseudo” Hamiltonian results, and an overlap matrix:

$$\tilde{H}_{ps} |\tilde{\Phi}_a\rangle = S \epsilon_a |\tilde{\Phi}_a\rangle , \quad S = 1 + \sum_{\mathbf{R}ij} |\tilde{p}_{\mathbf{R}i}\rangle (\langle \phi_{\mathbf{R}i} | \phi_{\mathbf{R}j} \rangle - \langle \tilde{\phi}_{\mathbf{R}i} | \tilde{\phi}_{\mathbf{R}j} \rangle) \langle \tilde{p}_{\mathbf{R}j}|$$

Only for norm-conserving PAW is $S = 1$: $\delta_{nm} = \langle \tilde{\Phi}_n | S | \tilde{\Phi}_m \rangle \stackrel{NC}{=} \langle \tilde{\Phi}_n | \tilde{\Phi}_m \rangle$

Basics of the PAW method III

The action of an (semi-local) AE operator O is retrieved by using a “pseudo” operator \tilde{O} with *one-centre* augmentation corrections:

$$\begin{aligned}\tilde{O} &= O + \sum_{\mathbf{R}ij} |\tilde{p}_{\mathbf{R}i}\rangle (\langle \phi_{\mathbf{R}i} | O | \phi_{\mathbf{R}j} \rangle - \langle \tilde{\phi}_{\mathbf{R}i} | O | \tilde{\phi}_{\mathbf{R}j} \rangle) \langle \tilde{p}_{\mathbf{R}j}| \\ \tilde{O} &= O + O^1 - \tilde{O}^1\end{aligned}$$

In practice all variational freedom is in the expansion coefficients of the orbitals (“pseudo wave functions”):

$$|\tilde{\Phi}_{n\mathbf{k}}\rangle = e^{i\mathbf{k}\cdot\mathbf{r}} |\tilde{u}_{n\mathbf{k}}(\mathbf{r})\rangle$$

The cell periodic part $|\tilde{u}_{n\mathbf{k}}\rangle$ is expanded in plane waves (n is band index):

$$|\tilde{u}_{n\mathbf{k}}(\mathbf{r})\rangle = \sum_{\mathbf{G}} c_{n\mathbf{k}\mathbf{G}} e^{i\mathbf{G}\cdot\mathbf{r}}$$

Basis set is truncated: $E_{\text{kin}} = \hbar^2 |\mathbf{G} + \mathbf{k}|^2 / (2m_e) < E_{\text{cut}}$

Basics of the PAW method IV

Let's see how this works for the kinetic energy:

$$\begin{aligned} -E_{\text{kin}} &= \sum_n f_n \langle \tilde{\Phi}_n | \left[\frac{\nabla^2}{2} + \sum_{\mathbf{R}ij} |\tilde{p}_{\mathbf{R}i}\rangle (\langle \phi_{\mathbf{R}i} | \frac{\nabla^2}{2} |\phi_{\mathbf{R}j}\rangle - \langle \tilde{\phi}_{\mathbf{R}i} | \frac{\nabla^2}{2} |\tilde{\phi}_{\mathbf{R}j}\rangle) \langle \tilde{p}_{\mathbf{R}j}| \right] |\tilde{\Phi}_n\rangle \\ &= \sum_n f_n \langle \tilde{\Phi}_n | \frac{\nabla^2}{2} |\tilde{\Phi}_n\rangle + (\langle \phi_{\mathbf{R}i} | \frac{\nabla^2}{2} |\phi_{\mathbf{R}j}\rangle - \langle \tilde{\phi}_{\mathbf{R}i} | \frac{\nabla^2}{2} |\tilde{\phi}_{\mathbf{R}j}\rangle) \sum_{\mathbf{R}ij} \sum_n f_n \langle \tilde{\Phi}_n | \tilde{p}_{\mathbf{R}i} \rangle \langle \tilde{p}_{\mathbf{R}j} | \tilde{\Phi}_n \rangle \\ &= \sum_n f_n \langle \tilde{\Phi}_n | \frac{\nabla^2}{2} |\tilde{\Phi}_n\rangle + (\langle \phi_{\mathbf{R}i} | \frac{\nabla^2}{2} |\phi_{\mathbf{R}j}\rangle - \langle \tilde{\phi}_{\mathbf{R}i} | \frac{\nabla^2}{2} |\tilde{\phi}_{\mathbf{R}j}\rangle) \sum_{\mathbf{R}ij} \rho_{ij\mathbf{R}} \\ &= -(\tilde{E}_{\text{kin}} + E_{\text{kin}}^1 - \tilde{E}_{\text{kin}}^1) \end{aligned}$$

The first term is easily calculated on the plane wave grid (with an FFT).

The **one-centre matrix elements of partial waves** are evaluated only once on a logarithmic grid inside the PAW spheres.

The **on-site density matrix ρ_{ij}** is easily calculated in reciprocal space. It can be accurately approximated in real space, using that the projector functions are short range.

Basics of the PAW method V

Now let's glance at the total energy $E_{\text{tot}} = \tilde{E}_{\text{tot}} - \tilde{E}_{\text{tot}}^1 + E_{\text{tot}}^1$.

The “plane wave” contribution:

$$\begin{aligned}\tilde{E} = & \sum_n f_n \langle \Phi_n | -\frac{\nabla^2}{2} | \Phi_n \rangle + E_{\text{xc}}[\tilde{n} + \hat{n} + \tilde{n}_c] + E_{\text{H}}[\tilde{n} + \hat{n}] \\ & + \int v_{\text{H}}[\tilde{n}_{Zc}] (\tilde{n}(\mathbf{r}) + \hat{n}(\mathbf{r})) d\mathbf{r} + U(\mathbf{R}, Z_{\text{ion}})\end{aligned}$$

n (\tilde{n}) is the (pseudo) valence charge density

\hat{n} is the compensation charge density: it is a smooth charge density that restores the correct number of electrons in the PAW sphere. This efficiently takes care of correct long-range electrostatics (well... you also need Ewald, of course).

n_c (\tilde{n}_c) is the (pseudo) core charge density.

$n_{Zc} = n_Z + n_c$, and \tilde{n}_{Zc} is a pseudized charge density with the same long-range effect.

Basics of the PAW method VI

The one-centre contributions are (\mathbf{R} summation suppressed):

$$\begin{aligned}\tilde{E}^1 = & \sum_{ij} \rho_{ij} \langle \tilde{\phi}_i | - \frac{\nabla^2}{2} | \tilde{\phi}_j \rangle + \overline{E_{xc}[\tilde{n}^1 + \hat{n} + \tilde{n}_c]} + \overline{E_H[\tilde{n}^1 + \hat{n}]} \\ & + \int_{\Omega_r} V_H[\tilde{n}_{Zc}](\tilde{n}^1(\mathbf{r}) + \hat{n}(\mathbf{r})) d\mathbf{r}\end{aligned}$$

$$E^1 = \sum_{ij} \rho_{ij} \langle \phi_i | - \frac{\nabla^2}{2} | \phi_j \rangle + \overline{E_{xc}[n^1 + n_c]} + \overline{E_H[n^1]} + \int_{\Omega_r} V_H[n_{Zc}] n^1(\mathbf{r}) d\mathbf{r}$$

Everything is on the radial grid inside the PAW sphere here, except the density matrix ρ_{ij} . But this density matrix determines the occupation of the augmentation channels:

$$n^1(\mathbf{r}) = \sum_{ij} \rho_{ij} \phi_i^*(\mathbf{r}) \phi_j(\mathbf{r}) , \quad \tilde{n}^1(\mathbf{r}) = \sum_{ij} \rho_{ij} \tilde{\phi}_i^*(\mathbf{r}) \tilde{\phi}_j(\mathbf{r})$$

G. Kresse, D. Joubert, Phys. Rev. B 59, 1764 (1999).

Basics of the PAW method VII

The KS Hamiltonian:

$$\tilde{H} = -\frac{\nabla^2}{2} + \sum_{ij} |\tilde{p}_i\rangle (\hat{D}_{ij} + D_{ij}^1 - \tilde{D}_{ij}^1) \langle \tilde{p}_j|$$

The KS equation with overlap:

$$\tilde{H}|\tilde{\Phi}_n\rangle = \tilde{S}\epsilon_n|\tilde{\Phi}_n\rangle , \quad \tilde{S} = 1 + \sum_{ij} |\tilde{p}_i\rangle (\langle\phi_i|\phi_j\rangle - \langle\tilde{\phi}_i|\tilde{\phi}_j\rangle) \langle\tilde{p}_j|$$

Note we have to sum over all sites \mathbf{R} .

The key references are:

*P.E. Blöchl, Phys. Rev. B **50**, 17953 (1994).*

*G. Kresse, D. Joubert, Phys. Rev. B **59**, 1764 (1999).*

Electric Field Gradients with PAW I

Traceless EFG tensor of derivatives of the field ($\alpha, \beta = x, y, z$):

$$V_{\alpha\beta} = \lim_{\mathbf{r} \rightarrow \mathbf{R}} (\partial_\alpha \partial_\beta - \frac{1}{3} \delta_{\alpha\beta} \nabla^2) v(\mathbf{r})$$

Potential is sum of soft, plane wave part and *one-centre* corrections:

$$\tilde{v}(\mathbf{r}) = v(\mathbf{r}) - \tilde{v}^1(\mathbf{r}) + v^1(\mathbf{r})$$

Just take the double derivative. For the plane wave part:

$$V_{\alpha\beta} = - \sum_{\mathbf{G}} \left(G_\alpha G_\beta - \delta_{\alpha\beta} \frac{|\mathbf{G}|^2}{3} \right) \tilde{v}(\mathbf{G}) e^{i\mathbf{G} \cdot \mathbf{R}}$$

The one-centre terms are like (only $l = 2$ terms survive):

$$v^1(\mathbf{r}) = \sum_{lm} v_{lm}^1(|\mathbf{r} - \mathbf{R}|) Y_{lm}(\mathbf{r} - \mathbf{R})$$

H.M. Petrilli, Blöchl, Blaha, Schwarz, Phys. Rev. B **57**, 14690 (1998).

Electric Field Gradients with PAW II

In practice: Bring the tensor $V_{\alpha\beta}$ locally to principal axes, such that:
 $|V_{zz}| > |V_{xx}| \geq |V_{yy}|$.

With NMR one probes the local $|V_{zz}|$ and asymmetry parameter η :

$$\eta = \frac{|V_{xx} - V_{yy}|}{|V_{zz}|}, \quad 0 \leq \eta \leq 1.$$

From experiment one does not directly obtain $|V_{zz}|$, but, instead, the so-called C_Q :

$$C_Q = eQC_{zz}/h$$

Here Q is the nuclear quadrupole moment. So for nuclei without a quadrupolar moment NMR cannot determine the EFG.

The moments one can get from the Pykkö table: *P. Pykkö. Mol. Phys. 99, 1617 (2001) & 106, 1964 (2008)*

Electric Field Gradients with PAW III

<http://www.chem.helsinki.fi/~pyykko/Q2008.pdf>

Electric Field Gradients with PAW IV

A test on TiO_2 (rutile), Ti EFGs in $\text{V}/\text{\AA}^2$, LDA

	frozen Ti states	V_{xx}	V_{yy}	V_{zz}
LAPW (Petrilli)		14.9	6.0	-20.9
PAW (Petrilli)	[Ne]	13.1	7.5	-20.6
PAW VASP St-PAW	[Ne]3s ² 3p ⁶	25.8	10.0	-35.8
PAW VASP St-PAW	[Ne]	15.6	7.4	-23.0
PAW VASP	[Ne]	14.8	6.5	-21.3
exp (Gabathuler)		14.9	7.9	-22.8
exp (Kanert)		13.4	8.6	-22.0

Take home message: EFGs require very high quality PAW data sets (potentials): completeness & semi-core.

Electric Field Gradients with PAW V

Summary:

- EFG calculations need ground state electron density only.
- EFG calculations require a “good completeness” of partial wave/projector functions set.
- semi-core states can be (often are) important.
- A very sensitive probe to structure.

Chemical shifts/shieldings: Basics I

Shielding (σ) and shift (δ) tensors of a nucleus N at site \mathbf{R} are defined:

$$\sigma_{\mathbf{R}\alpha\beta} = -\delta_{\mathbf{R}\alpha\beta} = -\frac{\partial B_{\mathbf{R}\alpha}^{\text{ind}}}{\partial B_{\beta}^{\text{ext}}} \underset{\text{linear}}{=} -\frac{B_{\mathbf{R}\alpha}^{\text{ind}}}{B_{\beta}^{\text{ext}}}$$

You calculate an absolute shielding, with - in principle - 9 independent cartesian components (α, β).

For a reference you need a separate calculation.

To go to NMR observables: symmetrize & bring to principal axes ($\sigma_{11} \leq \sigma_{22} \leq \sigma_{33}$).

$$\text{isotropic shielding} = \sigma_{\text{iso}} = (\sigma_{11} + \sigma_{22} + \sigma_{33})/3$$

$$\text{span} = \Omega = \sigma_{33} - \sigma_{11}$$

$$\text{skew} = \kappa = 3(\sigma_{22} - \sigma_{\text{iso}})/\Omega$$

J. Mason, Solid State Nucl. Magn. Reson. 2, 285 (1993).

Chemical shifts/shieldings: Basics II

In experiment you typically probe a chemical shielding difference, i.e., you have a *reference*. You then look at a chemical *shift*:

$$\delta_{\text{iso}}[N] = \delta_{\text{ref}}[N] - \sigma_{\text{iso}}[N]$$

where $\delta_{\text{ref}}[N] = -\sigma_{\text{ref}}[N]$ of the nucleus N in a system in well-defined state (this is usually a good approximation).

In calculation you can do the same thing, or do a fit, for a set of well-defined systems for which experimental shifts are known:

$$\delta_{\text{iso}}^{\text{exp}}[N] = \delta_{\text{ref}}[N] - m\sigma_{\text{iso}}^{\text{calc}}[N]$$

Now δ_{ref} and m are fit parameters. They both depend on N , and on the “level of theory” (and on the basis set).

From AE Hamiltonian to shielding

The AE electronic Hamiltonian:

$$H = \frac{1}{2m_e} \left(\mathbf{p} - \frac{e}{c} \mathbf{A}_0 \right)^2 + eV(\mathbf{r}) , \quad \mathbf{p} = \frac{\hbar}{i} \nabla$$

$V(\mathbf{r})$ is potential of positive nuclei, \mathbf{A}_0 is the vector potential of the external applied field:

$$\mathbf{A}_0 = \frac{1}{2} \mathbf{B}_{\text{ext}} \times \mathbf{r}$$

This is the symmetric gauge. Of course, there is gauge freedom.

Solve for the eigenstates $|\psi_i\rangle$ of H . The induced current is:

$$\mathbf{j}_{\text{ind}}(\mathbf{r}) = \overbrace{\frac{e\hbar}{m_e} \text{Im} \sum_n^{\text{occ}} [\psi_n^* \nabla \psi_n]}^{\text{paramagnetic}} - \overbrace{\frac{e^2}{m_e c} \mathbf{A}(\mathbf{r}) \rho(\mathbf{r})}^{\text{diamagnetic}} , \quad \rho(\mathbf{r}) = \sum_n^{\text{occ}} |\psi_n|^2$$

It gives an induced field via Biot-Savart:

$$\mathbf{B}_{\text{ind}}(\mathbf{R}') = \frac{1}{c} \int \frac{\mathbf{j}_{\text{ind}}(\mathbf{r}) \times (\mathbf{R}' - \mathbf{r})}{|\mathbf{R}' - \mathbf{r}|^3} d^3 r$$

Towards GIPAW I

The AE Hamiltonian requires too large basis sets... goto PAW: remove core and smooth wave functions, *transform operators*. Hamiltonian:

$$H^{\text{PAW}} = \frac{p^2}{2m_e} + \tilde{\nu}_{\text{eff}} + \sum_{\mathbf{R}ij} |\tilde{p}_{\mathbf{R}i}\rangle (\hat{D}_{ij} + D_{ij}^1 - \tilde{D}_{ij}^1) \langle \tilde{p}_{\mathbf{R}j}|$$

Retaining terms linear in \mathbf{B}_{ext} :

$$\begin{aligned} H^{\text{PAW}} &= H_{\mathbf{A}_0=0}^{\text{PAW}} - \frac{e}{m_e c} \mathbf{A}_0(\mathbf{r}) \cdot \mathbf{p} \\ &\quad - \frac{e}{m_e c} \sum_{\mathbf{R}ij} |\tilde{p}_{\mathbf{R}i}\rangle \left(\langle \phi_{\mathbf{R}i} | \mathbf{A}_0(\mathbf{r}) \cdot \mathbf{p} | \phi_{\mathbf{R}j} \rangle - \langle \tilde{\phi}_{\mathbf{R}i} | \mathbf{A}_0(\mathbf{r}) \cdot \mathbf{p} | \tilde{\phi}_{\mathbf{R}j} \rangle \right) \langle \tilde{p}_{\mathbf{R}j}| \end{aligned}$$

And an analogous expression for the current operator \mathbf{J} .

These expressions have gauge problems in both the *plane wave basis* and the *local partial wave basis*. Remember $\mathbf{A} \sim \mathbf{r}$.

Towards GIPAW II

In a formal sense the gauge problem arises from damage, done by the PAW, to the phase change the orbitals acquire upon translation.

Let's translate our KS Hamiltonian:

$$H = \frac{1}{2m_e} \left(\mathbf{p} - \frac{e}{c} \mathbf{A}_0 \right)^2 + eV(\mathbf{r} - \mathbf{T}) , \quad \mathbf{p} = \frac{\hbar}{i} \nabla$$

The eigenstate changes:

$$\psi(\mathbf{r}) \Rightarrow \psi^T(\mathbf{r}) = e^{(ie/2\hbar c)(\mathbf{B} \times \mathbf{T}) \cdot \mathbf{r}} \psi(\mathbf{r} - \mathbf{T})$$

because

$$\begin{aligned} & (\mathbf{p} - \frac{e}{c} \mathbf{A}_0) \psi^T(\mathbf{r}) \\ &= e^{i(\dots)} \mathbf{p} \psi(\mathbf{r} - \mathbf{T}) + \frac{\hbar}{i} \frac{ie}{2\hbar c} (\mathbf{B} \times \mathbf{T}) e^{i(\dots)} \psi(\mathbf{r} - \mathbf{T}) - \frac{e}{c} \frac{\mathbf{B} \times \mathbf{r}}{2} e^{i(\dots)} \psi(\mathbf{r} - \mathbf{T}) \\ &= e^{i(\dots)} \left(\mathbf{p} - \frac{e}{c} \mathbf{A}_0(\mathbf{r} - \mathbf{T}) \right) \psi(\mathbf{r} - \mathbf{T}) \end{aligned}$$

Solution: introduce a phase twist of projector functions (and partial waves) that restores the phase change.

Towards GIPAW III

The problem is solved by the **Gauge-Including PAW** (GIPAW).

In a formal sense: the phase change of the eigenfunctions upon translation is restored *via* partial waves and projector functions.

$$|\psi_n\rangle = |\tilde{\psi}_n\rangle + \sum_{\mathbf{R}i} e^{(ie/2\hbar c)\mathbf{A}_0(\mathbf{R}) \cdot \mathbf{r}} \left(|\phi_{\mathbf{R}i}\rangle - |\tilde{\phi}_{\mathbf{R}i}\rangle \right) \overbrace{\langle \tilde{p}_{\mathbf{R}i}| e^{-(ie/2\hbar c)\mathbf{A}_0(\mathbf{R}) \cdot \mathbf{r}} \tilde{\psi}_n\rangle}^{\langle \tilde{p}_{\mathbf{R}i}|}$$

Informal: the gauge-origin is locally shifted onto the nucleus in each PAW sphere, so the strength of the perturbation is minimized.

$$H^{\text{GIPAW}} = H_{\mathbf{A}_0=0}^{\text{PAW}} - \frac{e}{m_e c} \mathbf{A}_0(\mathbf{r}) \cdot \mathbf{p} \\ - \frac{e}{m_e c} \sum_{\mathbf{R}ij} |\tilde{p}_{\mathbf{R}i}\rangle \left(\langle \phi_{\mathbf{R}i} | \mathbf{A}_0(\mathbf{r}-\mathbf{R}) \cdot \mathbf{p} | \phi_{\mathbf{R}j} \rangle - \langle \tilde{\phi}_{\mathbf{R}i} | \mathbf{A}_0(\mathbf{r}-\mathbf{R}) \cdot \mathbf{p} | \tilde{\phi}_{\mathbf{R}j} \rangle \right) \langle \tilde{p}_{\mathbf{R}j}|$$

Analogous to GIAO with atomic orbitals.

C.J. Pickard, F. Mauri, Phys. Rev. B **63**, 245101 (2001).

Towards GIPAW IV

The Hamiltonian:

$$H^{\text{GIPAW}} = H_{\mathbf{A}_0=0}^{\text{PAW}} - \frac{e}{m_e c} \mathbf{A}_0(\mathbf{r}) \cdot \mathbf{p}$$
$$- \frac{e}{m_e c} \sum_{\mathbf{R}ij} |\bar{\tilde{p}}_{\mathbf{R}i}\rangle \left(\langle \phi_{\mathbf{R}i} | \mathbf{A}_0(\mathbf{r}-\mathbf{R}) \cdot \mathbf{p} | \phi_{\mathbf{R}j} \rangle - \langle \tilde{\phi}_{\mathbf{R}i} | \mathbf{A}_0(\mathbf{r}-\mathbf{R}) \cdot \mathbf{p} | \tilde{\phi}_{\mathbf{R}j} \rangle \right) \langle \bar{\tilde{p}}_{\mathbf{R}j} |$$

And the current operator:

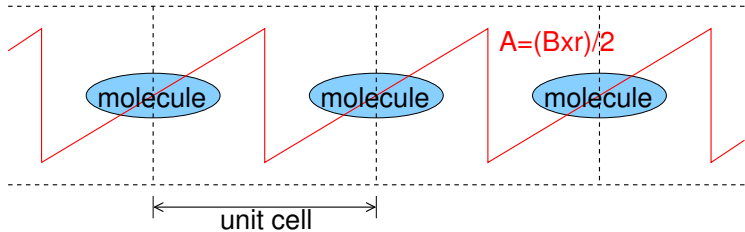
$$\mathbf{J}^{\text{GIPAW}}(\mathbf{r}) = \mathbf{J}(\mathbf{r}) + \sum_{\mathbf{R}ij} |\bar{\tilde{p}}_{\mathbf{R}i}\rangle \left(D_{\mathbf{R}ij}^1[\mathbf{J}^{\text{in}}] - \tilde{D}_{\mathbf{R}ij}^1[\mathbf{J}^{\text{in}}] \right) \langle \bar{\tilde{p}}_{\mathbf{R}j} | ,$$

$$D_{\mathbf{R}ij}^1[\mathbf{J}^{\text{in}}] = \langle \phi_{\mathbf{R}i} | \left\{ \frac{e\hbar}{2im_e} (\nabla|\mathbf{r}\rangle\langle\mathbf{r}| + |\mathbf{r}\rangle\langle\mathbf{r}|\nabla) - \frac{e^2}{m_e c} \mathbf{A}_0(\mathbf{r}-\mathbf{R}) |\mathbf{r}\rangle\langle\mathbf{r}| \right\} |\phi_{\mathbf{R}j} \rangle$$

Gauge problems in one-center terms have now been removed.
Gauge problems in the plane-wave basis are still present.

A simple working molecular scheme I

- GIPAW only (no hybrids)
- finite field, no perturbation theory
- hence, saw-tooth \mathbf{A}_0 because of periodic boundary conditions
- hence, only molecules.

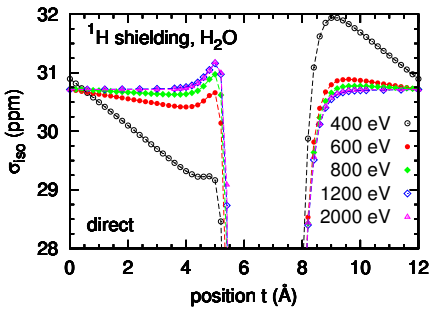
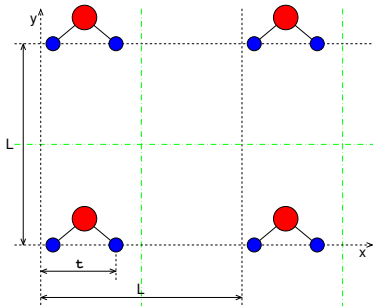


Recipe: (1) switch on \mathbf{A}_0 , (2) solve self-consistent problem, obtain eigenfunctions, (3) use those to calculate the current \mathbf{j} , (4) obtain induced field from Biot-Savart.

F. Vasconcelos, G.A. de Wijs, R.W.A. Havenith, M. Marsman, G. Kresse, J. Chem. Phys. 139, 014109 (2013)

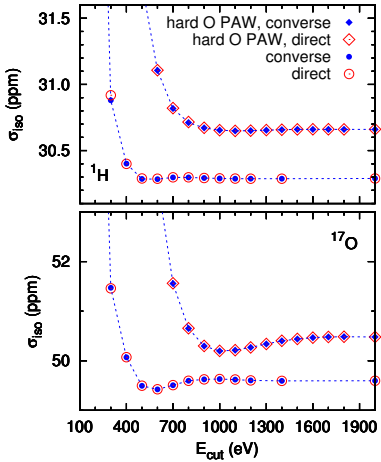
A simple working molecular scheme II

Plane-wave gauge problem: diamagnetic and paramagnetic shielding have different rates of converge with basis set size.



The gauge origin is at $t = 0$. With increasing kinetic energy cutoff E_{cut} the gauge problem disappears. Note the effect of the jump in \mathbf{A}_0 halfway the box.

A simple working molecular scheme III



PBE	augm.	$\sigma(^1\text{H})$	$\sigma(^{17}\text{O})$
standard O	no	30.84	49.49
hard O	no	31.33	50.37
standard O	yes	30.34	49.60
hard O	yes	30.71	50.48
Dalton		30.76	50.58

Valence only shieldings,
Dalton: quantum-chemical code, GIAO with
aug-cc-pCV5Z

Hard O: more complete set of partial waves (3d reference), smaller radii r_c .

augm.: 2-centre corrections for induced field \mathbf{B}^{ind} .

Note: one can get good numbers, for the wrong reasons.

Dalton, a molecular electronic structure program, Release 2.0 (2005), see
<http://www.kjemi.uio.no/software/dalton/dalton.html>

GIPAW linear response for solids I

- AE theory developed by Mauri et al. in the 1990s, extended to GIPAW in 3rd millenium: Yates, Pickard & Mauri.
- Based on perturbation theory. To first order in the magnetic field:

$$\begin{aligned} \mathbf{j}_{\text{ind}}^{(1)}(\mathbf{r}) = & \sum_i^{\text{occ}} \left(2\text{Re}\{\langle \bar{\psi}_i^{(0)} | \bar{\mathbf{J}}^{(0)}(\mathbf{r}) | \bar{\psi}_i^{(1)} \rangle \} \right. \\ & - \sum_j^{\text{occ}} \langle \bar{\psi}_i^{(0)} | \bar{\mathbf{J}}^{(0)}(\mathbf{r}) | \bar{\psi}_j^{(0)} \rangle \langle \bar{\psi}_j^{(0)} | \bar{\mathbf{S}}^{(1)} | \bar{\psi}_i^{(0)} \rangle \\ & \left. + \langle \bar{\psi}_i^{(0)} | \bar{\mathbf{J}}^{(1)}(\mathbf{r}) | \bar{\psi}_i^{(0)} \rangle \right) \end{aligned}$$

These are plane waves on the soft grid (so should have a tilde).
The $|\bar{\psi}_i^{(1)}\rangle$ is the first-order variation projected in the empty sub-space:

$$|\bar{\psi}_i^{(1)}\rangle = G(\epsilon_0)(\bar{H}^{(1)} - \epsilon^{(0)} \bar{\mathbf{S}}^{(1)})|\bar{\psi}_i^{(0)}\rangle , \quad G(\epsilon_0) = \sum_{e \in \text{empty}} \frac{|\bar{\psi}_e^{(0)}\rangle \langle \bar{\psi}_e^{(0)}|}{\epsilon - \epsilon_e}$$

GIPAW linear response for solids II

- The finite field approach is incompatible with periodic boundary conditions
- Perturbation theory problematic for uniform field (ill-defined matrix elements of perturbation). Solution:
 - (a) modulate the external field, $\mathbf{B} \rightarrow \mathbf{B}e^{i\mathbf{q} \cdot \mathbf{r}}$, and take the long-wave length limit: $\mathbf{q} \rightarrow 0$. Or ...
 - (b) modulate the position operator,

$$(\mathbf{r} - \mathbf{r}') \cdot \hat{\mathbf{u}}_i = \lim_{q \rightarrow 0} \frac{1}{2q} \left\{ e^{iq\hat{\mathbf{u}}_i \cdot (\mathbf{r} - \mathbf{r}')} - e^{-iq\hat{\mathbf{u}}_i \cdot (\mathbf{r} - \mathbf{r}')} \right\}$$

This leads to the following form of the current density:

$$\mathbf{j}_{\text{ind}}(\mathbf{r}') = \lim_{q \rightarrow 0} \frac{1}{2q} \{ \mathbf{S}(\mathbf{r}', q) - \mathbf{S}(\mathbf{r}', -q) \} + \mathbf{j}^{(1)}(\mathbf{r}')$$

We need all directions: around each \mathbf{k} -point we get a star of $\mathbf{k} + \mathbf{q}$ -points. One takes a sufficiently small, but finite q .

GIPAW linear response for solids III

- The para- and diamagnetic current densities have a different convergence rate w.r.t. the plane wave basis. The results are not invariant upon translation. This is cured with the generalized f -sum rule. One writes the “diamagnetic current” also with the paramagnetic current and a Green’s function. For the norm-conserving case (sum over occupied states)::

$$i \sum_o \langle \bar{\Psi}_0^{(0)} | [E, O] | \bar{\Psi}_0^{(0)} \rangle = 4 \sum_o \text{Re}[\langle \bar{\Psi}_0^{(0)} | OG(\epsilon_0) \frac{1}{i} [E, \bar{H}^{(0)}] | \bar{\Psi}_0^{(0)} \rangle]$$

where $\langle \Phi' | O | \Phi \rangle = -\langle \Phi | O | \Phi' \rangle$ and $\langle \Phi' | E | \Phi \rangle = \langle \Phi | E | \Phi' \rangle$

One takes $E = \mathbf{r}$ and O the paramagnetic current density (on the grid or as one-centre correction).

- no 2-centre corrections: often good approximation, see later.

*F. Mauri, B. G. Pfrommer, S. G. Louie, Phys. Rev. Lett. **77**, 5300 (1996),*

*C. J. Pickard, F. Mauri, Phys. Rev. B **63**, 245101 (2001),*

*J. R. Yates, C. J. Pickard, F. Mauri, Phys. Rev. B **76**, 024401 (2007).*

GIPAW linear response for solids IV

A look at the formulas... Biot-Savart is not affected, the current is written as:

$$\mathbf{j}^{\text{ind}}(\mathbf{r}) = \mathbf{j}_{\text{bare}}(\mathbf{r}) + \overbrace{\mathbf{j}_{\Delta p}(\mathbf{r}) + \mathbf{j}_{\Delta d}(\mathbf{r})}^{\text{one-centre augmentation}}$$

The diamagnetic one-centre only depends on the non-perturbed wave functions: similar as before.

The other 2 require the first-order change of the wave functions, e.g.:

$$\mathbf{j}_{\text{bare}}(\mathbf{r}) = \lim_{q \rightarrow 0} \frac{\mathbf{S}_{\text{bare}}(\mathbf{r}, q) - \mathbf{S}_{\text{bare}}(\mathbf{r}, -q)}{2q} + \mathbf{j}_{\text{bare}, Q_R}(\mathbf{r})$$

$$\begin{aligned} \mathbf{S}_{\text{bare}}(\mathbf{r}, q) &= \frac{2}{cN_k} \sum_{i=x,y,z} \sum_{o,\mathbf{k}}^{\text{occ}} \text{Re} \left[\frac{1}{i} \langle \tilde{u}_{o,\mathbf{k}} | \mathbf{J}_{\mathbf{k},\mathbf{k}+\mathbf{q}_i}^p(\mathbf{r}) G_{\mathbf{k}+\mathbf{q}_i}(\epsilon_{o,\mathbf{k}}) \mathbf{B}^{\text{ext}} \times \hat{\mathbf{u}}_i \cdot \mathbf{v}_{\mathbf{k}+\mathbf{q}_i}(\epsilon_{o,\mathbf{k}}) | \tilde{u}_{o,\mathbf{k}} \rangle \right. \\ &\quad \left. - \sum_{o'}^{\text{occ}} \langle \tilde{u}_{o,\mathbf{k}} | \mathbf{J}_{\mathbf{k},\mathbf{k}+\mathbf{q}_i}^p | \tilde{u}_{o',\mathbf{k}+\mathbf{q}_i} \rangle \langle \tilde{u}_{o',\mathbf{k}+\mathbf{q}_i} | \mathbf{B}^{\text{ext}} \times \hat{\mathbf{u}}_i \cdot \mathbf{s}_{\mathbf{k}+\mathbf{q}_i,\mathbf{k}} | \tilde{u}_{o,\mathbf{k}} \rangle \right] \end{aligned}$$

J. R. Yates, C. J. Pickard, F. Mauri, Phys. Rev. B **76**, 024401 (2007).

GIPAW linear response for solids V

$$\mathbf{j}_{\text{bare}}(\mathbf{r}) = \lim_{q \rightarrow 0} \frac{\mathbf{S}_{\text{bare}}(\mathbf{r}, q) - \mathbf{S}_{\text{bare}}(\mathbf{r}, -q)}{2q} + \mathbf{j}_{\text{bare, QR}}(\mathbf{r})$$

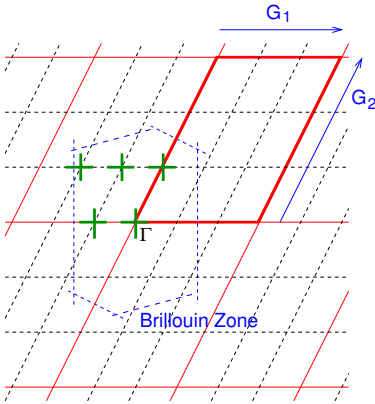
$$\begin{aligned} \mathbf{S}_{\text{bare}}(\mathbf{r}, q) = & \frac{2}{cN_k} \sum_{i=x,y,z} \sum_{o,\mathbf{k}}^{\text{occ}} \text{Re} \left[\frac{1}{i} \langle \tilde{u}_{o,\mathbf{k}} | \mathbf{J}_{\mathbf{k},\mathbf{k}+\mathbf{q}_i}^p(\mathbf{r}) \mathbf{G}_{\mathbf{k}+\mathbf{q}_i}(\epsilon_{o,\mathbf{k}}) \mathbf{B}^{\text{ext}} \times \hat{\mathbf{u}}_i \cdot \mathbf{v}_{\mathbf{k}+\mathbf{q}_i}(\epsilon_{o,\mathbf{k}}) | \tilde{u}_{o,\mathbf{k}} \rangle \right. \\ & \left. - \sum_{o'}^{\text{occ}} \langle \tilde{u}_{o,\mathbf{k}} | \mathbf{J}_{\mathbf{k},\mathbf{k}+\mathbf{q}_i}^p | \tilde{u}_{o',\mathbf{k}+\mathbf{q}_i} \rangle \langle \tilde{u}_{o',\mathbf{k}+\mathbf{q}_i} | \mathbf{B}^{\text{ext}} \times \hat{\mathbf{u}}_i \cdot \mathbf{s}_{\mathbf{k}+\mathbf{q}_i,\mathbf{k}} | \tilde{u}_{o,\mathbf{k}} \rangle \right] \end{aligned}$$

- Long wavelength limit: $q \rightarrow 0$, on a **cartesian star** around all \mathbf{k} points:
 $\mathbf{q}_i = q \hat{\mathbf{u}}_i$. q is finite and input of calculation.
- Response calculation: the **Green function** “virtually” sums over the empty states e :

$$G_{\mathbf{k}}(\epsilon) = \sum_e^{\text{empty}} \frac{|\tilde{u}_{e,\mathbf{k}}\rangle \langle \tilde{u}_{e,\mathbf{k}}|}{\epsilon - \epsilon_{e,\mathbf{k}}}$$

- Green function is not explicitly calculated, but its action is obtained by iteratively solving a so-called Sternheimer equation.
- Complications due to lifting the NC constraint are substantial.

GIPAW linear response for solids VI



Brillouin zone integration is summation over grid. Time reversal symmetry is used. Beware: not all symmetry operations of the lattice map the stars onto themselves! The choice of cartesian directions matters.

GIPAW linear response for solids VII

Sternheimer, the idea

Unperturbed problem has been solved.

$$H^{(0)}|\psi_n^{(0)}\rangle = \epsilon_n|\psi_n^{(0)}\rangle$$

Now apply first-order (in B^{ext}) perturbation:

$$H \rightarrow H^{(0)} + H^{(1)} \quad \text{and} \quad |\psi\rangle \rightarrow |\psi_n^{(0)}\rangle + |\psi_n^{(1)}\rangle$$

You obtain $\psi_n^{(1)}$ via the Green function:

$$|\psi_n^{(1)}\rangle = G(\epsilon_n)H^{(1)}|\psi_n^{(0)}\rangle = \sum_{\mathbf{e}}^{\text{empty}} \frac{|\psi_{\mathbf{e}}^{(0)}\rangle \langle \psi_{\mathbf{e}}^{(0)}|}{\epsilon_n - \epsilon_{\mathbf{e}}} H^{(1)}|\psi_n^{(0)}\rangle$$

Multiply with $(\epsilon_n - H^{(0)})\dots$

GIPAW linear response for solids VIII

Multiply with $(\epsilon_n - H^{(0)})$:

$$(\epsilon_n - H^{(0)})|\psi_n^{(1)}\rangle = (\epsilon_n - H^{(0)}) \sum_e^{\text{empty}} \frac{|\psi_e^{(0)}\rangle\langle\psi_e^{(0)}|}{\epsilon_n - \epsilon_e} H^{(1)} |\psi_n^{(0)}\rangle =$$
$$\sum_e^{\text{empty}} \frac{\epsilon_n - \epsilon_e}{\epsilon_n - \epsilon_e} |\psi_e^{(0)}\rangle\langle\psi_e^{(0)}| H^{(1)} |\psi_n^{(0)}\rangle = \left(1 - \sum_o^{\text{occ}} |\psi_o^{(0)}\rangle\langle\psi_o^{(0)}|\right) H^{(1)} |\psi_n^{(0)}\rangle$$

Use completeness to project in the empty subspace. Result: An equation with only occupied states for the single unknown set $|\psi_n^{(1)}\rangle$ which can be iteratively solved. No sum over empty states.

Beware: in general GIPAW this is more complicated, as the overlap matrix $\mathbf{S} \neq \mathbf{I}$, and the Green function G and its argument ϵ live at different \mathbf{k} -points.

GIPAW linear response for solids IX

From the current, we have to go to the induced field *via* Biot-Savart.
On the plane wave grid this is easy:

$$\mathbf{B}_{\text{ind}}(\mathbf{R}) = \frac{4\pi i}{c} \sum_{\mathbf{G} \neq 0} \frac{\mathbf{G} \times \mathbf{j}_{\text{ind}}(\mathbf{G})}{G^2} e^{i\mathbf{G} \cdot \mathbf{R}},$$

The one-center contributions yield currents in the PAW spheres around *all nuclei*. Only the field that results at the center of each sphere is considered. Fields due to augmentations at other PAW spheres are neglected. *Often this is a good approximation.*

For the diamagnetic field strength parameters, e.g.,

$$\langle \phi_{\mathbf{R}i} | -\frac{(\mathbf{B}_{\text{ext}} \times (\mathbf{r} - \mathbf{R}))}{2c} \times \frac{(\mathbf{R} - \mathbf{r})}{c|\mathbf{R} - \mathbf{r}|^3} | \phi_{\mathbf{R}j} \rangle - \langle \tilde{\phi}_{\mathbf{R}i} | \dots | \tilde{\phi}_{\mathbf{R}j} \rangle$$

The partial waves are products of radial functions and spherical harmonics. Such terms can be done with Glebsch-Gordan.

GIPAW linear response for solids X

Alternatively, the current density strengths can be replaced with smooth (Bessel) functions times spherical harmonics, with the *same* multipole expansions. E.g., for the diamagnetic current density

$$-\phi_{\mathbf{R}i}^*(\mathbf{r})\phi_{\mathbf{R}j}(\mathbf{r}) \frac{(\mathbf{B}_{\text{ext}} \times (\mathbf{r} - \mathbf{R}))}{2c} \rightarrow \sum_{LM} I_{\mathbf{R}ij}^{LM} g_L(|\mathbf{r} - \mathbf{R}|) Y_{LM}(\mathbf{R})$$

These can be represented on the plane wave grid, and account for the fields from other PAW spheres. This may lead to non-trivial *paramagnetic* corrections (Vasconcelos *et al.*, see below).

GIPAW linear response for solids XI

The total (absolute) shielding is:

$$\sigma_{\mathbf{R}\alpha\beta} = \sigma_{\mathbf{R}\alpha\beta}^{\text{GIPAW}} + \delta_{\alpha\beta}\sigma_{\mathbf{R}}^{\text{core}} + \sigma_{\alpha\beta}^{\text{surface}}$$

$\sigma_{\mathbf{R}\alpha\beta}^{\text{GIPAW}}$ Shielding due to electrons treated in PAW for the infinite crystal. Typically shielding due to valence electrons.

$\sigma_{\mathbf{R}}^{\text{core}}$ Shielding due to the other (“core”) electrons. Diagonal, one number for each element. Nearly constant (in this gauge, Gregor *et al.*, J. Chem. Phys. **111**, 1815 (1999)).

$\sigma_{\alpha\beta}^{\text{surface}}$ Macroscopic, shape dependent field due to surface currents. Constant on microscopic length scale, i.e.

$B_{\alpha}^{\text{ind}}(\mathbf{G} = 0)/B_{\beta}^{\text{ext}}$. Obtained from macroscopic magnetic susceptibility $\chi_{\alpha\beta}$. For a sphere:

$$\sigma_{\alpha\beta}^{\text{surface}} = -\frac{8\pi}{3}\chi_{\alpha\beta}$$

χ is also calculated in GIPAW linear response, using an Ansatz with the proper AE limit. This is a second order finite difference in the BZ.

Comparing implementations

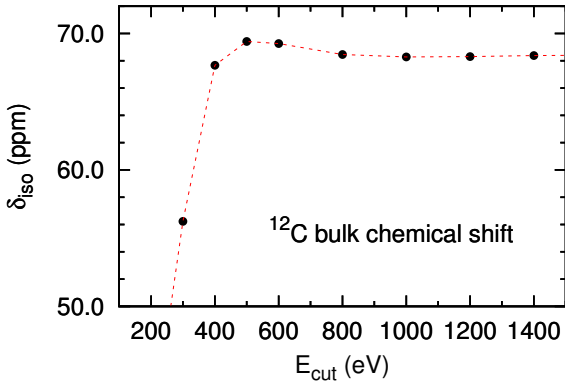
New VASP implementation: tests on Aluminophosphate crystals

		Quantum-ESPRESSO			VASP		
		σ_{iso} (ppm)	Ω (ppm)	κ	σ_{iso} (ppm)	Ω (ppm)	κ
Berlinite	Al	260.90	9.39	-0.79	258.04	9.39	-0.76
	P	606.16	9.25	0.17	604.07	9.35	0.16
	O	95.52	89.70	-0.89	94.06	88.94	-0.88
	O	93.79	93.27	-0.89	92.11	92.45	-0.88
Aluminium cyclo-hexaphosphate	Al	205.17	4.37	-0.49	202.61	4.35	-0.47
	P	583.45	207.57	-0.34	580.57	206.11	-0.34
	P	590.45	202.08	-0.33	587.72	200.86	-0.33
	P	588.01	207.35	-0.26	585.11	206.19	-0.26
	O	109.13	90.21	-0.38	108.42	87.27	-0.38
	O	112.26	90.29	-0.38	111.46	87.27	-0.38
	O	110.41	87.41	-0.71	109.45	84.39	-0.71
	O	118.35	79.21	-0.65	117.62	76.21	-0.65
	O	114.82	89.72	-0.28	114.03	86.64	-0.28
	O	121.13	80.26	-0.29	120.30	77.40	-0.29
	O	142.12	104.52	-0.99	140.99	104.10	-0.97
	O	151.01	89.45	-0.57	149.90	88.56	-0.60
	O	153.23	87.53	-0.61	152.10	86.75	-0.63
low-cristobalite	Al	258.40	5.27	0.24	255.41	5.35	0.24
	P	603.99	15.17	0.58	602.02	15.25	0.60
	O	90.14	102.81	-0.91	89.43	100.99	-0.91
	O	88.50	103.61	-0.88	87.92	101.63	-0.88

*Q-ESPRESSO: P. Giannozzi, S. Baroni, N. Bonini, et al., J. Phys.: Condens. Matter **21**, 395502 (2009), <http://www.quantum-espresso.org>*

Illustration on diamond I

Plane wave basis set convergence



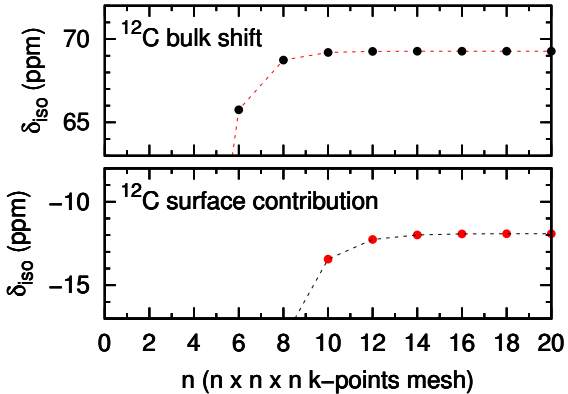
Typically cutoffs larger than default are needed:

Default: $E_{\text{cut}} = \text{ENCUT} = 414$ eV, converged within 2 ppm,

For very good convergence: 800 eV. (note: it should be ^{13}C)

Illustration on diamond II

k-point convergence



Convergence with **k**-points for a Γ -centered mesh ($E_{\text{cut}} = 600$ eV).
Surface (χ derived) contribution converges slower.

Converse approach to NMR shielding I

The shielding tensor $\sigma_{\mathbf{R}\alpha\beta}$ at site \mathbf{R} is related to the energy of putting a virtual magnetic dipole $\mathbf{m}_{\mathbf{R}}$ at that site.

$$\delta_{\alpha\beta} - \sigma_{\mathbf{R}\alpha\beta} = \frac{\partial(B_{\alpha}^{\text{ext}} + B_{\mathbf{R}\alpha}^{\text{ind}})}{\partial B_{\beta}^{\text{ext}}} = -\frac{\partial}{\partial B_{\beta}^{\text{ext}}} \frac{\partial E}{\partial m_{\mathbf{R}\alpha}} = -\frac{\partial}{\partial m_{\mathbf{R}\alpha}} \frac{\partial E}{\partial B_{\beta}^{\text{ext}}} =$$
$$\Omega \frac{\partial M_{\beta}}{\partial m_{\mathbf{E}\alpha}} = \Omega \frac{\partial(m_{\beta\mathbf{R}}/\Omega + M_{\beta}^{\text{ind}})}{\partial m_{\mathbf{R}\alpha}} = \delta_{\alpha\beta} + \Omega \frac{\partial M_{\beta}^{\text{ind}}}{\partial m_{\mathbf{R}\alpha}}$$

(Beware: Ω = volume, $\delta_{\alpha\beta}$ = Kronecker delta)

Calculus and definitions do the rest... so you apply:

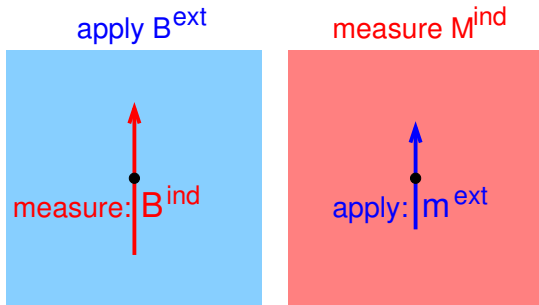
$$\mathbf{A}_{\mathbf{R}} = \frac{\mathbf{m}_{\mathbf{R}} \times (\mathbf{r} - \mathbf{R})}{|\mathbf{r} - \mathbf{R}|^3} \text{ and calculate } \mathbf{m}^{\text{ind}} = \Omega \mathbf{M}^{\text{ind}} = \frac{1}{2c} \int \mathbf{r} \times \mathbf{j}_{\text{ind}} d^3r$$

For infinite systems, obtaining \mathbf{M}^{ind} is a story in itself...

T. Thonhauser, D. Ceresoli, A.A. Mostofi, N. Marzari, R. Resta,
D. Vanderbilt, J. Chem. Phys. **131**, 101101 (2009).

Converse approach to NMR shielding II

A cartoon:



$$\sigma_{\mathbf{R}\alpha\beta} = -\frac{\partial B_{\mathbf{R}\alpha}^{\text{ind}}}{\partial B_{\beta}^{\text{ext}}} = -\frac{\partial m_{\beta}^{\text{ind}}}{\partial m_{\mathbf{R}\alpha}}$$

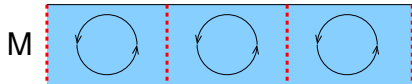
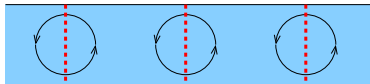
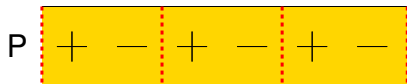
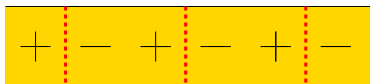
The induced field (left) and applied moment (right) both live in the same point.

“Modern” theory of orbital magnetisation I

Magnetisation = dipole moment per volume Ω :

$$\mathbf{M} = \frac{\mathbf{m}}{\Omega} = \frac{1}{2c\Omega} \int \mathbf{r} \times \mathbf{J}(\mathbf{r}) d^3r$$

Problematic in a periodic system, how to choose unit cell... ?



In fact, in both cases *the position operator \mathbf{r} is ill-defined.*

“Modern” theory of orbital magnetisation II

Solution: Start with a finite chunk, use *localized* Wannier functions, and take the thermodynamic limit.

$$\mathbf{M} = -\frac{1}{2c\Omega N_c} \sum_{i=1}^{N_c N_b} \langle \mathbf{w}_i | \mathbf{r} \times \mathbf{v} | \mathbf{w}_i \rangle , \quad \mathbf{v} = i[H, \mathbf{r}]$$

This can be split:

$$\mathbf{M} = \mathbf{M}_{LC} + \mathbf{M}_{IC}$$

LC = Local Circulation, interior well-behaved contribution:

$$\mathbf{M}_{LC} = -\frac{1}{2c\Omega N_c} \sum_{n\mathbf{R}} \langle n\mathbf{R} | (\mathbf{r} - \mathbf{R}) \times \mathbf{v} | n\mathbf{R} \rangle$$

IC = Itinerant Circulation, surface shape *independent* surface contribution.

D. Ceresoli, T. Thonhauser, D. Vanderbilt, R. Resta, Phys. Rev. B 74, 024408 (2006), and others.

“Modern” theory of orbital magnetisation III

In terms of *delocalized* Bloch functions:

$$\mathbf{M}_{LC} = \frac{1}{16c\pi^3} \text{Im} \sum_n \int_{BZ} \langle \partial_{\mathbf{k}} u_{n\mathbf{k}} | \times H_{\mathbf{k}} | \partial_{\mathbf{k}} u_{n\mathbf{k}} \rangle d^3k$$

$$\mathbf{M}_{IC} = \frac{1}{16c\pi^3} \text{Im} \sum_{nn'} \int_{BZ} \epsilon_{nn'\mathbf{k}} \langle \partial_{\mathbf{k}} u_{n\mathbf{k}} | \times | \partial_{\mathbf{k}} u_{n'\mathbf{k}} \rangle d^3k$$

The $|u_{n\mathbf{k}}\rangle$ are the cell-periodic parts. Note these expressions depend on their phase. The \mathbf{k} -derivatives are available in many solid state electronic structure codes.

Note: this is an AE expression. It is valid for any well-behaved Hamiltonian, so also for that of a norm-conserving pseudopotential:

$$\mathbf{M}_{ps} = \frac{1}{16c\pi^3} \text{Im} \sum_n^{\text{occ}} \int_{BZ} \langle \partial_{\mathbf{k}} \tilde{u}_{n\mathbf{k}} | \times (\tilde{H}_{\mathbf{k}} + \epsilon_{n\mathbf{k}}) | \partial_{\mathbf{k}} \tilde{u}_{n\mathbf{k}} \rangle d^3k$$

This opens a route to efficient shielding calculations...

Converse approach to crystal shielding I

Hellmann-Feynman:

$$M_\beta = -\frac{\partial E}{\partial B_\beta} \stackrel{\text{HF}}{=} -\left\langle \frac{\partial H^{\text{AE}}}{\partial B_\beta} \right\rangle_{\mathbf{B}=0} = -\left\langle \frac{\partial H^{\text{GIPAW}}}{\partial B_\beta} \right\rangle_{\mathbf{B}=0}$$

Also:

$$\mathbf{M} = -\frac{1}{2c\Omega} \int \mathbf{r} \times \mathbf{J}^{\text{AE}} d^3r = -\frac{1}{2c\Omega} \sum_n^{\text{occ}} \langle \psi_n | \mathbf{r} \times \mathbf{v}^{\text{AE}} | \psi_n \rangle , \quad \mathbf{v}^{\text{AE}} = i[H^{\text{AE}}, \mathbf{r}]$$

$$\mathbf{M} \neq \tilde{\mathbf{M}} = -\frac{1}{2c\Omega} \int \mathbf{r} \times \mathbf{J}^{\text{ps}} d^3r = -\frac{1}{2c\Omega} \sum_n^{\text{occ}} \langle \psi_n | \mathbf{r} \times \mathbf{v}^{\text{ps}} | \psi_n \rangle , \quad \mathbf{v}^{\text{ps}} = i[H^{\text{GIPAW}}, \mathbf{r}]$$

Write expressions for the **red terms** (\mathbf{r} unbound), subtracting gives $\mathbf{M} - \tilde{\mathbf{M}}$: this is *short-range*, i.e. one-centre corrections with only differences $\mathbf{r} - \mathbf{R}$.

For $\tilde{\mathbf{M}}$ use the modern theory. The “ \mathbf{r} ”-problem is solved.

Note: Also here a GIPAW is needed, for the *induced* (vanishing) uniform field.

D. Ceresoli, N. Marzari, M. Lopez, T. Thonhauser, Phys. Rev. B 81, 184424 (2010)

Converse approach to crystal shielding II

Features:

- ☺ Relatively easy to program, $\partial_{\mathbf{k}} \tilde{U}_{n\mathbf{k}}$ and partial wave derivatives for one-center terms available in many solid-state codes.
- ☺ Finite field, no linear-response calculation needed, no Sternheimer.
- ☺ Relatively easy to apply for post-DFT, contrary to Sternheimer, but... ☹
- ☹ Supercell approach, finite field.
- ☹ Atom-by-atom, but can start from pre-converged run, the perturbation is very small ... ☺
- ☹ True crystal magnetisation, to account for surface effects separately.

Benchmarks

The VASP linear response GIPAW periodic implementation compared to FLAPW:

- **Molecules** in *large* periodically repeated cells ($16 \times 16 \times 16$ and $17 \times 17 \times 17 \text{ \AA}^3$). Non-relativistic. Also compared to quantum chemical GIAO in vacuum with DALTON. *Dalton, a molecular electronic structure program, Release Dalton2011 (2011)*, see <http://daltonprogram.org>
- **Crystals**: shieldings and susceptibilities. Also compared to experiment. Scalar-relativistic.
- Identical geometries (no relaxation). PBE functional.
- Standard and very accurate PAW data sets (potentials): hard and often norm-conserving.

*G.A. de Wijs, R. Laskowski, P. Blaha, R.A.W. Havenith, G. Kresse, M. Marsman, J. Chem. Phys. **146**, 064115 (2017)*

Two center-corrections to the current. Same VASP compared to DALTON GAIO and accurate multi-wavelet results (Jensen *et al.*, PCCP **18**, 21145 (2016)). Only molecules & identical geometries, PBE.

*F. Vasconcelos, G.A. de Wijs, R.W.A. Havenith, M. Marsman, G. Kresse, J. Chem. Phys. **139**, 014109 (2013) & unpublished*

Benchmarks: Molecules, isotropic shieldings

PBE	Wien2k	VASP		other GIPAW	DALTON2011, NREL, aug-cc-pCVXX			
	NREL	opt.-NREL	standard		5Z	QZ	TZ	DZ
Al shieldings								
[AlH ₄] ⁻		477.50	483.93		477.94	478.23	480.89	492.93
Al ₂ H ₆	402.8	404.60	411.13	405.79	404.25	404.49	406.96	415.62
AlH ₃	249.7	251.03	258.54	251.02	250.24	250.46	254.22	259.22
Si shieldings								
Si ₂ H ₆	436.9	439.98	443.01	440.70	439.38	439.65	443.27	460.86
SiH ₄	431.6	434.30	437.68	436.06	433.63	433.92	437.76	458.40
Si ₂ H ₄	235.9	239.55	240.56	236.69	238.28	238.53	241.53	252.13
SiH ₂	-533.4	-526.34	-523.91	-526.69	-530.20	-530.34	-527.12	-539.66
P shieldings								
P ₄	858.8	862.54	864.49	8861.16	861.56	861.68	862.31	864.60
PH ₃		575.77	579.61	5577.47	576.50	576.82	580.02	596.71
P ₂ H ₄	517.0	519.46	522.93	5519.68	520.11	520.42	523.61	541.00
H ₃ PO ₄	281.8	283.87	292.51	2285.73	284.65	285.00	289.31	308.91
PF ₃	153.9	156.05	156.58	1158.02	155.72	155.94	159.74	174.83
P ₂	-306.0	-301.98	-318.00	-318.62	-301.79	-301.32	-298.10	-288.67
F shieldings								
CASTEP ^a								
CH ₃ F		450.91	452.45	452.1	451.65	451.74	452.26	452.52
HF	399.0	398.64	398.97	398.8	399.98	400.21	401.02	402.91
C ₆ F ₆		314.99	313.72	310.6	316.73	317.14	319.20	324.28
CH ₂ F ₂		299.98	297.81	298.7	301.56	301.98	304.13	308.81
CF ₄	211.2	210.51	205.01	207.0	212.35	212.94	216.14	221.75
PF ₃	176.8	173.76	172.08		178.20	178.90	183.41	202.56
CFCI ₃		117.49	114.92	113.2	120.02	120.79	124.94	132.21
NF ₃	-62.5	-63.18	-74.86	-73.5	-59.52	-58.33	-52.04	-39.55
F ₂	-293.4	-292.54	-307.14	-296.3	-288.21	-286.56	-276.99	-261.85

^a CASTEP shieldings from A. Sadoc, M. Body, C. Legein, et al., Phys. Chem. Chem. Phys. **13**, 18539 (2011)

Benchmarks: Solids, isotropic shieldings

	WIEN2k	σ_{iso} VASP		other GIPAW	δ_{iso} expt. ^d	WIEN2k	χ_m VASP		
		optim.	standard				optim.	standard	expt. ^d
F shieldings									
NaF	393.98	389.21	392.86	395.8 ^a	-224.2	-16.0	-10.9	-11.6	-15.6
LiF	370.12	368.14	367.65	369.3 ^a	-204.3	-10.8	-9.1	-7.7	-10.1
InF ₃	365.55	363.17	365.02		-209.2	-54.8	-43.4	-35.7	
MgF ₂	362.93	362.59	362.92	362.7 ^a	-197.3	-23.5	-24.1	-38.8	-22.7
α -AlF ₃	335.32	334.06	334.51		-172.0	-30.1	-28.3	-24.9	-13.9
GaF ₃	312.51	307.23	310.63		-171.2	-42.6	-29.5	-28.2	
KF	271.08	270.41	271.27	268.1 ^a	-133.3	-23.4	-25.1	-23.2	-23.6
RbF	223.34	223.07	226.54	221.3 ^a	-90.9	-31.6	-31.0	-34.0	-31.9
CaF ₂	220.72	219.99	220.02	220.0 ^a	-108.0	-25.8	-26.7	-22.7	-28
SrF ₂	216.17	216.05	220.17	215.3 ^a	-87.5	-34.4	-33.6	-34.6	-37.2
TlF	148.92	146.10	152.06		-19.1	-50.7	-30.6	-42.8	-44.4
CsF	127.01	126.94	136.24	136.3 ^a	-11.2	-44.3	-40.9	-44.9	-44.5
BaF ₂	126.05	128.19	156.10	151.9 ^a	-14.3	-44.8	-42.2	-51.7	-51
MAD(F)	0.00	1.76	4.41	5.0		0.0	4.9	6.4	

^a A. Sadoc, M. Body, C. Legein, et al., *Phys. Chem. Chem. Phys.* **13**, 18539 (2011)

^b D. S. Middlemiss, F. Blanc, C. J. Pickard, C. P. Grey, *J. Magn. Reson.* **204**, 1 (2010)

^c M. Profeta, F. Mauri, and C. J. Pickard, *J. Am. Chem. Soc.* **125**, 541 (2003)

^d various experiments

Benchmarks: Solids, isotropic shieldings

	σ_{iso} VASP				δ_{iso} expt. ^d	χ_m VASP			
	WIEN2k	optim.	standard	other GIPAW		WIEN2k	optim.	standard	expt. ^d
	O shieldings								
BeO	234.17	232.59	231.44	232.2 ^b	26	-12.6	-11.2	-10.8	-11.9
SiO ₂	214.21	213.83	213.95		41	-24.3	-24.9	-23.7	-28.6
MgO	201.77	200.25	200.82	198.0 ^b	47	-15.8	-18.3	-15.8	-10.2
BaSnO ₃	86.08	85.09	96.61	98.0 ^b	143	-73.1	-61.5	-70.4	
CaO	-145.56	-146.05	-145.30	-156.6 ^c	294	-11.4	-13.4	-15.7	-15.0
BaZrO ₃	-174.74	-171.75	-160.04	-172.8 ^b	376	-39.3	-39.6	-62.9	
SrO	-213.16	-218.29	-215.53	-205.2 ^b	390	-16.5	-17.6	-22.4	-35
SrTiO ₃	-290.61	-289.75	-289.14	-287.3 ^b	465	-10.0	-9.8	-36.5	
BaTiO ₃	-361.06	-359.49	-348.40	-347.4 ^b	523	-12.4	-11.0	-48.4	
BaO	-481.43	-483.71	-458.46	-444.3 ^b	629	-17.3	-18.4	-30.7	-29.1
MAD(O)	0.00	1.76	7.48	10.2		0.0	2.2	11.5	

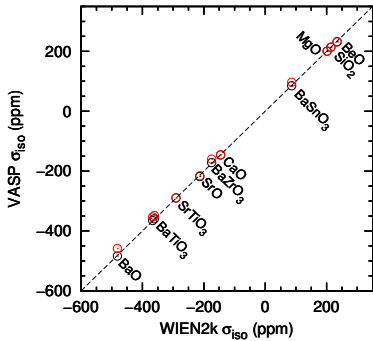
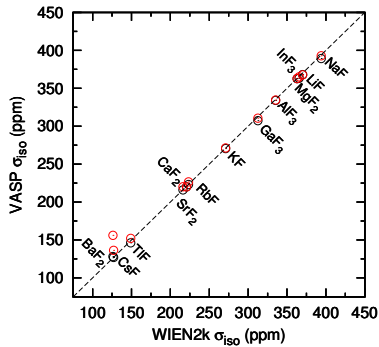
^aA. Sadoc, M. Body, C. Legein, et al., *Phys. Chem. Chem. Phys.* **13**, 18539 (2011)

^bD. S. Middlemiss, F. Blanc, C. J. Pickard, C. P. Grey, *J. Magn. Reson.* **204**, 1 (2010)

^cM. Profeta, F. Mauri, and C. J. Pickard, *J. Am. Chem. Soc.* **125**, 541 (2003)

^dvarious experiments

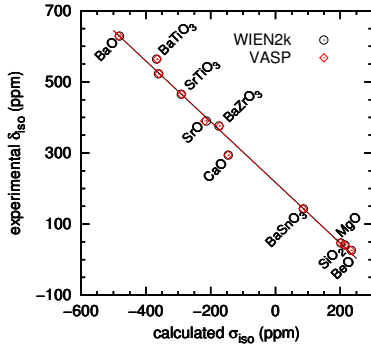
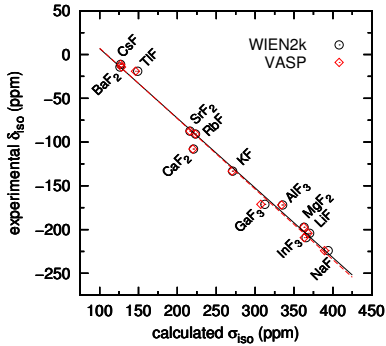
Benchmarks: Solids, isotropic chemical shifts



Black (red): optimized (standard) PAW data sets

Standard Cs and Ba show significant deviations

Benchmarks: Solids, isotropic chemical shifts



Ca *d*-state problem (*Profeta et al, JACS 126, 1694 (2001)*)

Fit:

$$\delta[\text{F}]_{\text{iso}}^{\text{exp}} = 86.47 - 0.7964 \sigma_{\text{iso}}^{\text{WIEN2k}}, \quad \delta[\text{O}]_{\text{iso}}^{\text{exp}} = 217.23 - 0.8546 \sigma_{\text{iso}}^{\text{WIEN2k}}$$

$$\delta[\text{F}]_{\text{iso}}^{\text{exp}} = 87.76 - 0.8056 \sigma_{\text{iso}}^{\text{VASP}}, \quad \delta[\text{O}]_{\text{iso}}^{\text{exp}} = 216.67 - 0.8558 \sigma_{\text{iso}}^{\text{VASP}}$$

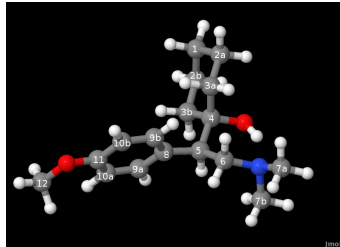
$$\delta[\text{F}]_{\text{iso}}^{\text{exp}} = 101.64 - 0.8429 \sigma_{\text{iso}}^{\text{VASP, std}}, \quad \delta[\text{O}]_{\text{iso}}^{\text{exp}} = 220.65 - 0.8724 \sigma_{\text{iso}}^{\text{VASP, std}}$$

Benchmarks: 2-centre contributions

- The augmentation currents from the *other* PAW spheres that give a contribution to the induced magnetic field: 1-centre contributions to the current felt in the induced field at other sites.
- Neglected in GIPAW papers of Yates, Pickard & Mauri. Often a very **good approximation**.
- However... it plays a non-trivial role for **H-shieldings**:
 - Double/triple bonds, e.g., C₂H₄, C₂H₂ (trade-off with hardness...)
 - Comparison with quantum-chemical calculations, i.e. *basis sets*.
- In VASP: multi-pole expansion of currents is represented on the plane wave grid.
- Illustration: venlafaxine molecule in PBE with aug-cc-pCVTZ (DALTON) and VASP.

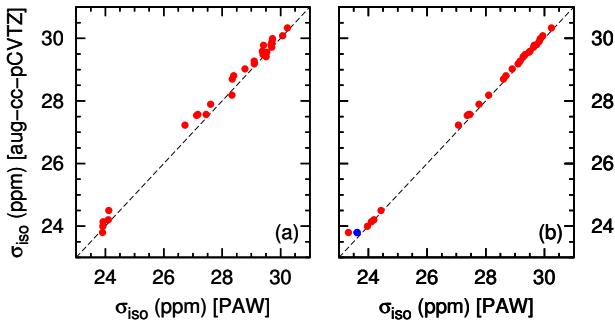
F. Vasconcelos, G.A. de Wijs, R.W.A. Havenith, M. Marsman, G. Kresse, J. Chem. Phys. 139, 014109 (2013)

Benchmarks: 2-centre contributions



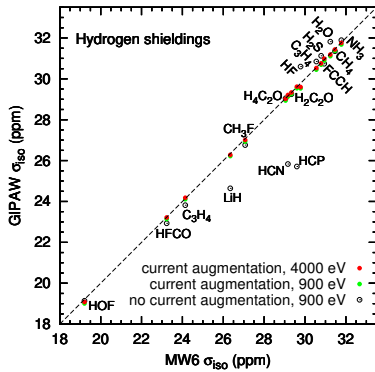
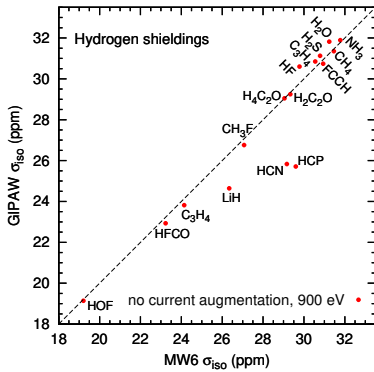
no augmentation

with augmentation



Benchmarks: 2-centre contributions

Significant effects for ^1H shieldings



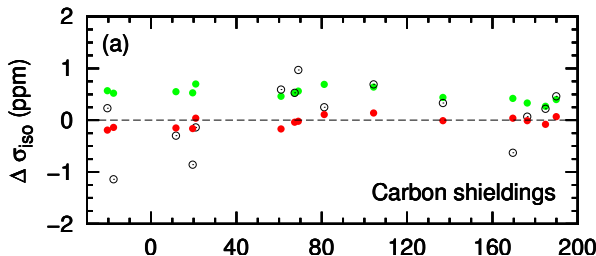
MW6: numerically exact, multi-wavelet benchmark from *S. R. Jensen, T. Flå, D. Jonsson, R. S. Monstad, K. Ruud, and L. Frediani, Phys. Chem. Chem. Phys.* **18**, 21145 (2016).

Accurate (hard) PAW data sets are needed.

Benchmarks: 2-centre contributions

Small effects for ^{13}C shieldings

$$\Delta\sigma_{\text{iso}} = \sigma_{\text{iso}}^{\text{GIPAW}} - \sigma_{\text{iso}}^{\text{MW6}}$$



Black: no current augmentation (900 eV), green: current augmentation (900 eV), red: current augmentation (4000 eV).

2-centre corrections reduce scatter.

Higher plane wave kinetic energy cutoff reduces average error.

Doing a calculation, linear response I

The 4 input files and run:

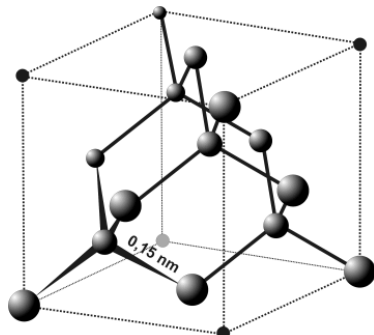
```
prompt$ ls
INCAR  KPOINTS  POSCAR  POTCAR
prompt$ mpiexec -np 8 ~/exe/vasp > STDOUT
prompt$ ls
EIGENVAL  DOSCAR  OSZICAR  POTCAR      XDATCAR
CHG        IBZKPT  OUTCAR   STDOUT
CHGCAR     INCAR   PCDAT    vasprun.xml
CONTCAR    KPOINTS POSCAR   WAVECAR
prompt$ more STDOUT OSZICAR OUTCAR
...
...
```

Doing a calculation, linear response II

You have to tell about the lattice vectors spanning the unit cell and where are the atoms.

```
prompt$ more POSCAR
fcc
 3.49800000
 0.5000  0.5000  0.0000
 0.0000  0.5000  0.5000
 0.5000  0.0000  0.5000
 2
C
 0.0000  0.0000  0.0000
 0.2500  0.2500  0.2500
prompt$
```

$$a = 3.489 \text{ \AA}$$



<http://commons.wikimedia.org/wiki/Diamond>

Doing a calculation, linear response III

You have to tell about the integration of the Brillouin zone.

```
prompt$ more KPOINTS
test
 0
G
 12 12 12
 0 0 0
prompt$
```

Here a $12 \times 12 \times 12$ regular mesh is put in the first unit cell of the reciprocal lattice. The Γ -point is included in this mesh.

The PAW projector sets are in a data-base:

```
prompt$ cat ~/database/PBE.52/C/POTCAR > POTCAR
prompt$
```

Selects a C data-set for the PBE exchange-correlation functional.

Doing a calculation, linear response IV

The file that controls the calculation:

```
prompt$ more INCAR
# inputs that require care
ISMEAR = 0; SIGMA= 0.1
PREC = A
EDIFF = 1E-12
ENCUT = 800

# GIPAW linear response inputs
LCHIMAG = .TRUE.      # default: .FALSE.
DQ = 0.003            #          0.001
NLSPLINE = .TRUE.     #          .FALSE.
ICHIBARE = 1           #          1
LNMR_SYM_RED = .FALSE. #          .FALSE.

# LREAL = A ; ISYM = -1 ; LWAVE = .FALSE.
```

Applications with VASP I

Cation (dis)order in III-V semiconductors:

- P.J. Knijn, P.J.M. van Bentum, E.R.H. van Eck, C.M. Fang, D.L.A.G. Grimminck, R.A. de Groot, R.W.A. Havenith, M. Marsman, W.L. Meerts, G.A. de Wijs, A.P.M. Kentgens, *A solid-state NMR and DFT study of compositional modulations in $Al_xGa_{1-x}As$* , Phys. Chem. Chem. Phys. **12**, 11517 (2010). Modelling the effect of disorder on EFGs in next-nearest neighbour shells.
- M. Goswami, P.J. Knijn, G.J. Bauhuis, J.W.G. Janssen, P.J.M. van Bentum, G.A. de Wijs, A.P.M. Kentgens, *Stripline ^{75}As NMR Study of Epitaxial III-V Semiconductor $Al_{0.5}Ga_{0.5}As$* , J. Phys. Chem. C **118**, 13394 (2014). Effect of structural relaxations on EFGs.
- P.J. Knijn, P.J.M. van Bentum, C.M. Fang, G.J. Bauhuis, G.A. de Wijs, A.P.M. Kentgens, *A multi-nuclear magnetic resonance and density functional theory investigation of epitaxially grown $InGaP_2$* , Phys. Chem. Chem. Phys. **18**, 21296 (2016). Chemical shifts of $In_xGa_{1-x}P_2$.

Organic crystals:

- C.M. Gowda, F. Vasconcelos, E. Schwartz, E.R.H. van Eck, M. Marsman, J.J.L.M. Cornelissen, A.E. Rowan, G.A. de Wijs, A.P.M. Kentgens, *Hydrogen bonding and chemical shift assignments in carbazole functionalized isocyanides from solid-state NMR and first-principles calculations*, Phys. Chem. Chem. Phys. **13**, 13082 (2011). Chemical shielding with converse approach, revealing weak bonds with NICS analysis.
- J.O. Brauckmann, P. Zolfaghari, R. Verhoef, E.A. Klop, G.A. de Wijs, A.P.M. Kentgens, *Structural Studies of Polyaramid Fibers: Solid-State NMR and First-Principles Modeling*, Macromolecules **49**, 5548 (2016). Assessing structural models comparing calculated and measured chemical shifts.

Methylammonium Lead Iodide:

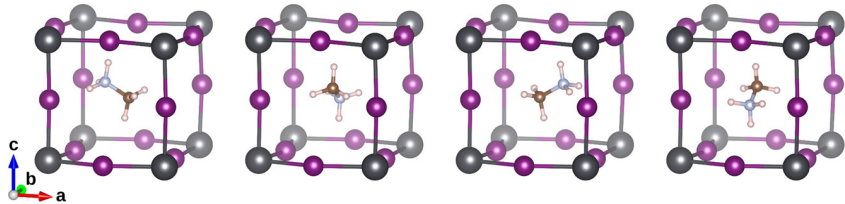
- W.M.J. Franssen, S.G.D. van Es, R. Dervişoğlu, G.A. de Wijs, A.P.M. Kentgens, *Symmetry, Dynamics, and Defects in Methylammonium Lead Halide Perovskites*, J. Phys. Chem. Lett. **8**, 61 (2017). See below.

Cation dynamics in MAPbI_3

Extremely “hot” photovoltaic perovskite material, $\text{CH}_3\text{NH}_3\text{PbI}_3$.

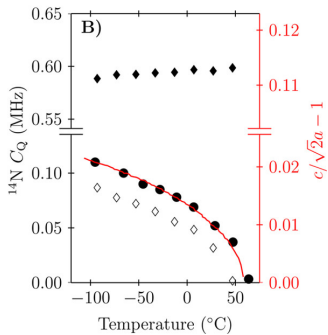
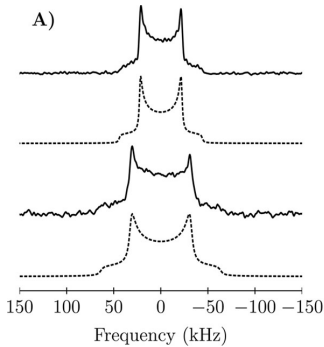
Increasing T : orthorhombic \rightarrow **tetragonal** \rightarrow cubic

Controversy about space group: polar $I4/cm$ or non-polar $I4/mcm$.



W.M.J. Franssen, S.G.D. van Es, R. Dervişoğlu, G.A. de Wijs, A.P.M. Kentgens, J. Phys. Chem. Lett. 8, 61 (2017)

Cation dynamics in MAPbI_3 II



Powder ^{14}N NMR: axial symmetry, $\eta = 0 \rightarrow$ non-polar.

DFT- C_Q modelling: only one MA ion in super cell, rest replaced by Cs^+ , optimize MA coordinates, fixed inorganic cage, experimental c/a ratios, average over four orientations consistent with non-polar $I4/mcm$.